

MSc Thesis Biosystems Engineering

Improving vision based classification between sugar beet and volunteer potato plants using regular plant spacing features

J.C.P. Boonman

December 2013



WAGENINGEN UNIVERSITY
WAGENINGEN UR

Improving vision based classification between sugar beet and volunteer potato plants using regular plant spacing features

Name course : Thesis Farm Technology
Number : FTE-80436
Study load : 36 credits
Date : December 2013

Student : Jan-Kees (J.C.P.) Boonman
Registration number: 90-08-02-098-040
Study programme : MSc Biosystems Engineering (MAB)

Supervisor : Dr. ir. Jan Willem (J.W.) Hofstee
Examiner : Prof. dr. ir. Eldert (E.J.) van Henten
Group : Farm Technology Group
Droevendaalsesteeg 1
6708 PB Wageningen
Tel: +31 (317) 48 29 80
E-mail: Office.FTE@wur.nl

Preface

This report is the result of my thesis work done for the MSc Biosystems Engineering at the Wageningen University. This thesis was carried out in collaboration with the Farm Technology Group. The aim of this thesis was to investigate the potential of the regular plant pattern features in a sugar beet crop, in order to improve the current vision based classification between sugar beet and volunteer potato plants. I've come to this subject because of my interest in precision farming, automation and programming.

In November 2012, I started working on this thesis. After I've stopped some periods to follow courses and work at the farm at home, I am glad that I can finish this thesis now. After all I can say that I never lost my interest in the topic and it made me more realise my big interest for precision farming.

I would like to thank my supervisor Jan Willem Hofstee for his good assistance, clear arrangements and time in guiding me to finish this thesis work. Also I would like to thank Eldert van Henten in advance for assessing my report. Furthermore I would like to give a thank to my study friends for the well-needed distraction from my thesis work every now and then. It helped me to go on with my work with a fresh mind. Finally I would like to thank my family and my girlfriend for their support and believe in me that I could complete my studies.

I hope that the knowledge gained from this thesis work can at least for a small amount contribute to a sustainable future of agriculture.

Jan-Kees Boonman
December 2013

Summary

Volunteer potatoes are one of the most important weeds in the cultivation of sugar beets. Having these volunteer potato plants can be a nest of diseases and harm the crop rotation. Therefore these plants should be removed, but for this no sophisticated method is available. In Nieuwenhuizen (2009) a machine was described that is able to automatically detect and control volunteer potato plants in a sugar beet crop. The accuracy of this machine was too low and improvements were needed. The current classification algorithm is only based on colour features. It was expected that adding new features would improve the classification accuracy. Therefore in this research the potential of the regular plant pattern of a sugar beet crop as classification feature was investigated.

The objective of this research was to estimate the position of the upcoming beet plant in the future beet row. The main question of this research was if by using the regular plant pattern, 68% of the next beet positions can be estimated with an accuracy of at most 3 cm. To estimate the position of the upcoming beet plant, the pattern in which the beets occur must be revealed from the previous underlying beet row. From the research of Nieuwenhuizen (2009) multiple image datasets were available. But because of the poor regularity of the plant pattern in these datasets, also simulated datasets were used.

Attempts with use of linear regression were stopped, since the exact positions of the individual beet plants in the previous beet row were needed. This appeared to be a problem to determine exactly. A more appropriate method was found to be the Fast Fourier Transformation. From this transformation the frequency and phase of a cosine wave can be deduced. The frequency was bounded to be determined from an a priori set interval corresponding to a possible range of sowing distances ranging from 15 to 25 cm. When overlaying the cosine wave to the original signal the peaks of it should correspond to the position of individual beets. The peaks of the extrapolated cosine wave correspond to the estimated position of the next beets in the future beet row.

Equally to Nieuwenhuizen a step size of 20 cm was used, meaning that every 20 cm the position(s) of the next beet plants in the future beet row were estimated. The positive part of the extrapolated cosine wave with an amplitude of 1 acted as probability distribution. The current frequency was smoothed by taking a weighted average of the current and previous determined frequencies. The accuracy of the estimate was determined in terms of a deviation between the estimated and actual beet position (ϵ) and in terms of the probability from the probability distribution at the actual beet position (P_{bp}), which were only determined when the actual beet was classified as found.

For the image datasets on average 70.5% of the actual next beets were found. For the simulated datasets this was 96.2%. The position of these found beets was estimated in the image datasets with an accuracy of on average 0.0 ± 3.7 cm. For the simulated datasets this was 0.1 ± 2.4 cm. Missing beet plants and volunteer potatoes in the previous underlying beet row both negatively influence the ability of this algorithm to estimate the next beet position.

Drawback of the algorithm was that no feedback was available that determined if the cosine wave corresponded to the original beet row signal. Therefore it occurred that the next beet positions were estimated on basis of a non-corresponding beet pattern.

To improve the current algorithm, first priority is to add a measure that determines the degree of similarity between the original intensity graph and the corresponding cosine wave. This degree can judge the relevance of the provided next beet position estimate. Eventually this method can be added to the current colour based classification algorithm.

Content

Preface.....	vii
Summary	ix
Content	xi
1 Introduction	1
1.1 General	1
1.2 Problem description.....	2
1.3 Objective	3
1.4 Research questions	4
1.5 Demarcation	4
1.6 Report structure	4
2 Literature	5
3 Materials and methods.....	11
3.1 Datasets	11
3.2 Image processing.....	11
3.3 Accuracy determination of plant distance	12
3.3.1 Image datasets	12
3.3.2 Measurement datasets.....	13
3.3.3 Plant distance histograms	14
3.4 Linear regression method to estimate future beet positions	15
3.4.1 Theory	15
3.4.2 Linear regression method in an online application.....	16
3.4.3 Probability distribution in beet row	18
3.4.4 Consideration about the linear regression method	19
3.5 Theory of the Fast Fourier transform	19
3.5.1 Theory	19
3.5.2 Filter mask.....	20
3.5.3 Non-discrete frequencies	22
3.6 Determination of sine wave frequency and phase	24
3.6.1 Simplified crop row simulation	24
3.6.2 Determine frequency	25
3.6.3 Determine phase	26
3.7 Application of next beet position estimation method on a crop row	27
3.7.1 Create intensity graph.....	27

Content

3.7.2	Estimate next beet position.....	28
3.7.3	Accuracy determination.....	30
3.7.4	Effect of missing beet plants	31
3.7.5	Effect of volunteer potato plant.....	31
4	Results	33
4.1	Image datasets	33
4.2	Metric accuracy	33
4.3	Accuracy determination over the crop row	35
4.4	Effect of missing beet plants	36
4.5	Effect of volunteer potato plant.....	38
5	Discussion	41
5.1	Literature	41
5.2	Materials and methods.....	41
5.3	Results	43
6	Conclusions	45
7	Recommendations	47
	References	49
	Appendix	i
	Appendix A	iii
	Appendix B	v
	Appendix C	vi
	Appendix D	x
	Appendix E.....	xiii
	Appendix F.....	xvi
	Appendix G	xvii
	Appendix H	xix
	Appendix I.....	xx

1 Introduction

1.1 General

Sugar beets are one of the major arable farming crops in The Netherlands. In 2012 an area of 72,724 hectares was cultivated with sugar beets (CBS, 2012). When growing a sugar beet crop, volunteer potato plants are an important weed. These volunteer potato plants are sprouted from tubers leftover from previous cropping seasons. Because no selective herbicides are available to remove the volunteer potato plants from a sugar beet field, the volunteer potato plants can become a nest of diseases and pests towards neighbouring potato fields. Also the crop rotation on the field is disturbed, when large amounts of volunteer potato plants are present.

Volunteer potato plants can appear when potatoes are present in the crop rotation. At harvest of this crop, small tubers will be sieved out and remain on the field. These small tubers can survive multiple seasons in the top soil layer, dependent on the species and weather conditions, and will sprout in a subsequent cropping season when conditions are favourable. Prevention against volunteer potatoes can be to minimize harvest losses, give tubers the opportunity to freeze in winter or plant potatoes species with low germination power (Veerman, 2003).

Currently the most effective method is to manually remove the volunteer potato plants from the crop, for instance by dipping the plant with glyphosate or pulling it out of the soil. Mechanised methods are available but are less effective, like spraying glyphosate with crop covers or dipping the volunteer potato plants with glyphosate by a pass of a roll on the basis of their greater height as compared to the crop. These removal actions are best carried out when the volunteer potato plants have a diameter of 10 cm (Campen, 2009). Each stem of the volunteer potato plant has to be handled with glyphosate to destroy it completely.

Sugar beets are planted with a precision drill with a standard row distance of 50 cm. A standard in-row plant distance is about 20 cm resulting in on average 100,000 beets per hectare. However, the optimum number of beet plants which will result in the maximum sugar yield and financial revenue, is about 80,000 plants per hectare (Figure 1). This actual lower plant number is common practise, because of missing plants due to non-germination, diseases or pests. Only when plant numbers per hectare drop below 60,000 plants, yield and revenue decrease substantially.

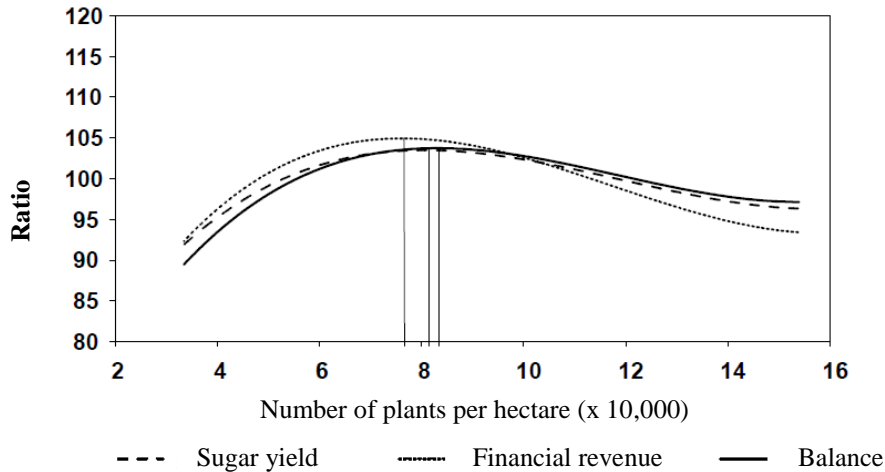


Figure 1: Influence of number of plants per hectare on ratios of sugar yield, financial revenue and balance. Balance indicates financial revenue minus the cost of seeds. Vertical lines indicate the optimum plant number for the three measures each. Translated from IRS (2000).

The current methods to remove volunteer potatoes are all labour consuming and/or not effective enough. Therefore a PhD research was carried out by Nieuwenhuizen (2009) to come up with a machine that is able to automatically detect and remove volunteer potato plants. This machine was able to control up to 83% of the volunteer potatoes, with 1.4% of unwanted controlled sugar beet plants.

1.2 Problem description

Current situation

Nieuwenhuizen (2009) did research to design and implement a solution to automatically detect and control volunteer potato plants in a sugar beet crop, but the control rate of 83% did not reach the requirement of 95% control of volunteer potato plants. Nieuwenhuizen only used colour features to make a distinction between volunteer potato and sugar beet plants. Other classification features as texture and planting distance were not investigated in this research.

In 2012 the Agrobot project proceeded the research of Nieuwenhuizen. The aim of the Agrobot project is to develop multisensory robots for agriculture, to offer a solution for current problems like the shortage of proper employment and soil compaction due to large machinery. The Agrobot project, in turn, is a part of the Smartbot project. This is a collaboration between 24 different partners from the Netherlands and Germany. One of the five demos that is developed in the Agrobot project, is a robot to detect and control volunteer potato plants in a sugar beet field. For this demo a Husky Robot is available, a sketch is shown in Figure 2. This robot will be equipped with a camera on the front and an actuator on the back, allowing to handle one crop row at a time.

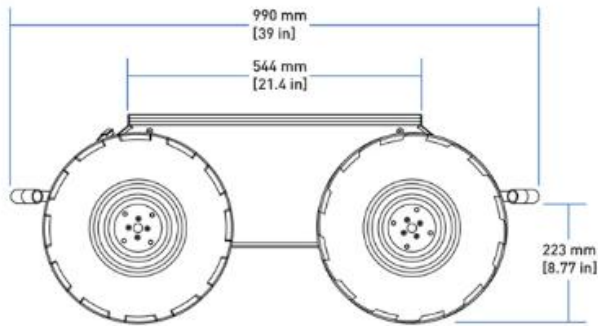


Figure 2: Side view of the Husky robot (ClearpathRobotics, 2013).

Vollebregt (2013) did research to enhance the classification by adding texture parameters. The improvements of this enhancement were little and further research is needed to use this classification feature. Jager (2013) has researched how natural light conditions can be normalized in an image, such that protection against natural light by using a cover would not be needed anymore. In this thesis a method is developed that adjusts colour images such that these are less dependent on variations in natural lighting conditions.

Summarized the current method needs improvements in the quality of detecting the volunteer potatoes and the Agrobot project requires a solution to implement the method on a small robot, in order to provide a practical solution to automatically detect and control volunteer potatoes in a sugar beet crop.

Desired situation

This thesis is part of the Agrobot project, for which the desired situation is to come up with an autonomous vehicle that is able to detect and control volunteer potatoes in a sugar beet crop. Classification is based on colour features supported with plant position and texture features. The robot handles one crop row at a time and adapts its speed to the frequency of present volunteer potato plants. Also the robot can deal with changing natural light conditions, such that a light cover is not required. The robot is able to control up to 95% of the volunteer potato plants and maximal 5% unwanted controlled sugar beet plants.

For this thesis the desired situation is that it is proven that the regularity of the plant pattern is an appropriate feature to add in the vision based classification between volunteer potato and sugar beet plants. The exact planting distance is not a priori information needed, since the algorithm is able to determine this by itself. This is a desired requirement, since the plant distance does not necessarily correspond with the setting of the sowing machine or the plant distance can simply be forgotten.

Problem definition

It is unknown if the regular sowing pattern is an appropriate feature to make an improvement to the classification between volunteer potato and sugar beet plants.

1.3 Objective

The objective of this research is to investigate the characteristics of the regular plant pattern of a sugar beet crop, in order to provide an estimate of the beet positions in the future beet row. This is called the next beet position estimate. To make this estimate, the regular beet pattern has to be extended from the

detected pattern in the current and previous area. The method is accepted to be sufficiently accurate if 68% of the next beet position estimates ($-\sigma \leq \mu \leq \sigma$) is within 3 cm of the true beet center point.

If the next beet estimation method is accepted, it could be added to the existing classification algorithm which is only based on colour features. A complete control of volunteer potato plants is desired before this method is applicable in practise. Therefore the objective is to improve the true negative classification, which indicates the percentage of correctly classified volunteer potato plants. This may be at the expense of a somewhat lower true positive classification, indicating the correctly classified sugar beets. But regarding Figure 1 the production and financial revenue of the cultivation of a sugar beet crop will in most cases not decline substantially when some sugar beet plants were controlled.

1.4 Research questions

The main research question is:

Can the regular sowing pattern of a sugar beet crop provide an estimate of the future beet position, in which 68% of the future beet position estimates is within 3 cm of the true beet center point?

Sub questions

- How regular is the plant pattern in a crop row?
- What methods can be used to detect a pattern in a crop row?
- To what extent can the algorithm handle an unknown sowing distance?
- What is the effect of missing beet plants on the next beet position estimate?
- What is the effect of plants that are not in the pattern on the next beet position estimate?

1.5 Demarcation

For this research only image datasets shall be used originating from the research by Nieuwenhuizen. These datasets contain top view images of three adjacent sugar beet crop rows with a random appearance of volunteer potato plants. These datasets originate from the years 2007 and 2008. So during this research no more image data is gathered in practise.

1.6 Report structure

After this introduction in Chapter 2 an overview is given of relevant work that was done in other researches before. In Chapter 3 two possible methods were described that are able to determine the pattern of the sugar beet plants. First the linear regression method is described. As it appeared that this method was not suitable, a switch was made to use the Fast Fourier Transformation. The results of using this method are shown in Chapter 4. Subsequently these results are discussed in Chapter 5 and the conclusions are drawn in Chapter 6. Some recommendations for future research are presented in Chapter 7.

2 Literature

In this chapter the outcome of a literature study is presented. Below an overview is given of the work of a number of researchers who did research in the same field as this research.

Nieuwenhuizen

The research by Nieuwenhuizen (2009) was part of his PhD thesis entitled '*Automated detection and control of volunteer potato plants*'. This thesis reports about the research done to develop an automated discrimination between volunteer potato plants in a sugar beet crop. It was found that with colour features a proper distinction could be made between the two different plants species. Under artificial light conditions an unsupervised adaptive Bayesian classifier was used, which was trained to adapt to different field conditions. At the end the machine was able to control 75 to 100% of the volunteer potato plants, improving with decreased travelling speed. On average this resulted in 1.4% unwanted controlled sugar beet plants. In Figure 3 an image and sketch of the machine is seen.

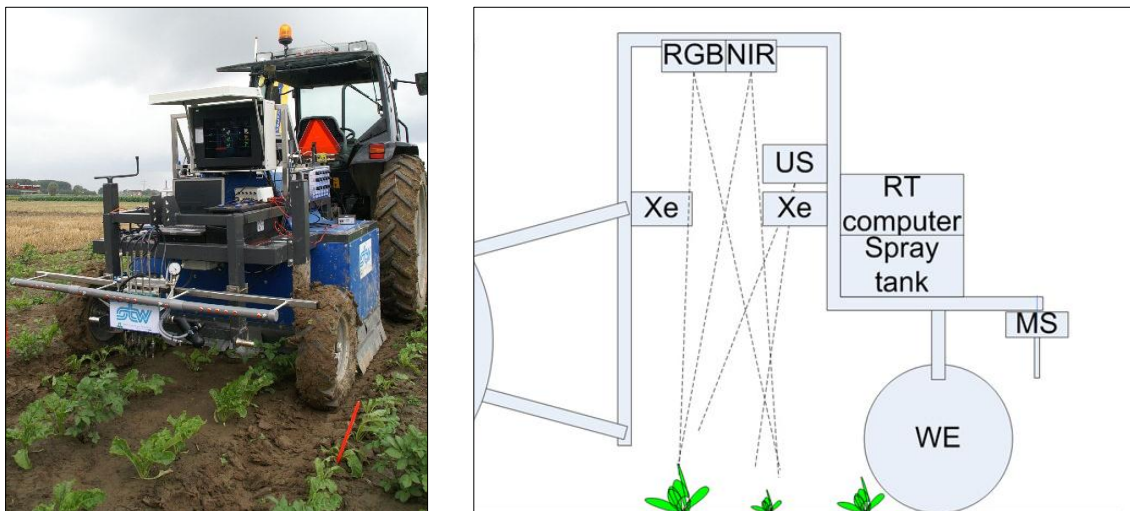


Figure 3: Image of machine attached to a tractor (left) and a schematic overview of the machine components (right). Cameras (RGB and NIR), artificial lighting (XE) and an ultrasonic height sensor (US) are mounted under the blue shed. Wheel encoder (WE) and micro sprayer (MS) as well as the computer are placed behind the shed.

In Table 1 the classification performances of the algorithm by Nieuwenhuizen are given. From the table it is seen that classification accuracy is varying considerably between the different datasets. This classification accuracy is determined as $\frac{TN+TP}{TN+FN+TP+FP}$. Special attention has to be given to the varying TN percentages, since this represents the volunteer potato plants that were classified as such. This classification is of importance, since it determines the amount of correctly controlled volunteer potato plants.

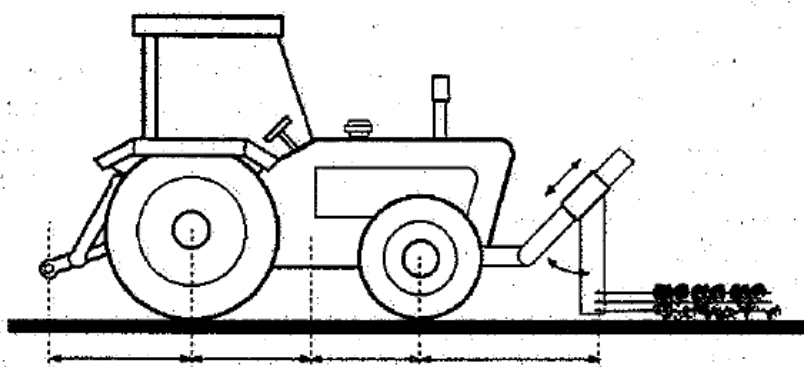
Table 1: Various datasets with classification results achieved by Nieuwenhuizen *et al.* (2009).

Dataset name	Ground truth	Result VP	Result SB	Classification accuracy
		TN	FP	
	VP	TN	FP	
	SB	FN	TP	
2008-05-28	VP	82.1	17.9	94.6
Clay soil	SB	4.0	96.0	
2008-05-30	VP	90.8	9.2	92.4
Clay soil	SB	7.4	92.6	
2008-06-02	VP	78.2	21.8	79.9
Clay soil	SB	19.8	80.2	
2008-05-28	VP	19.7	80.3	71.2
Sand soil	SB	25.3	74.7	
2008-05-30	VP	4.0	96.0	60.7
Sand soil	SB	37.9	62.1	

Bontsema

In Bontsema *et al.* (1991) a method is described to identify individual crop plants in a row crop. For this the regular pattern of the crop is used. The appearance of weeds is assumed to be random. The Fourier analysis is considered to be a useful tool, since it is able to filter out a periodicity in a signal. If the crop plants are positioned in a regular pattern, as can be reached with a precision seeder or a planting machine, crop plants will appear in a single frequency in the crop row. So if plants can be detected, the frequency of the crop plants can be filtered out.

Measurements were performed on a real row of sugar beet plants with a sensor mounted in front of a tractor (Figure 4). The sensor consists of three pairs of sensors that were mounted at different heights besides the crop row. On one side of the crop row infrared lights and on the other side photoelectric cells were placed. These cells do or do not catch infrared light, indicating the presence of a plant at that certain position. The result of a measurement are shown in Figure 5.

Figure 4: Tractor with sensor mounted on the front used to perform the measurements. (Bontsema *et al.*, 1991).

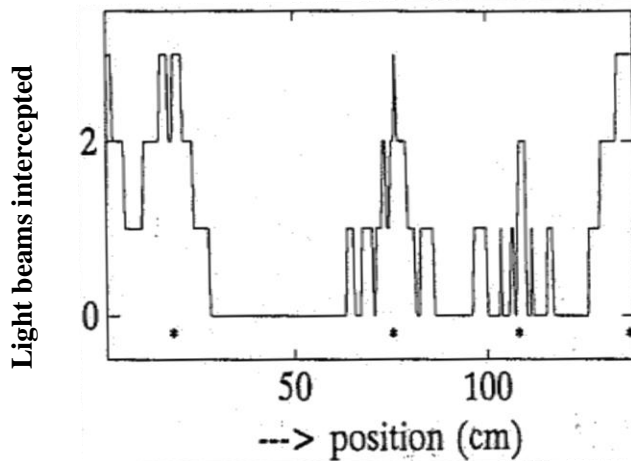


Figure 5: Measured data of a row of sugar beets. Dots indicate the position of individual beet plants. No weeds were present. (Bontsema *et al.*, 1991).

To perform Fourier analysis the Fast Fourier Transformation (FFT) is used. This resulted in a frequency domain spectrum of the signal from Figure 5, shown in Figure 6.

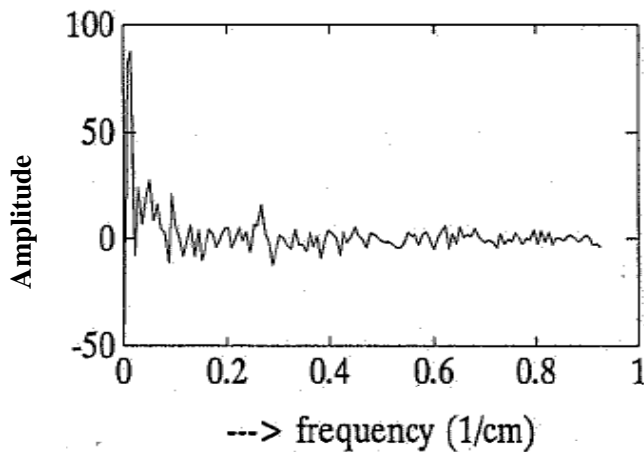


Figure 6: Frequency spectrum of measured data from Figure 5. (Bontsema *et al.*, 1991).

From this spectrum all frequencies larger than 0.3 cm^{-1} were set to zero. Taking the inverse FFT of this spectrum resulted in the graph in Figure 7. It is clear that the peaks correspond to the position of the individual beet plants (dots), thus it is possible by this method to locate individual beet plants.

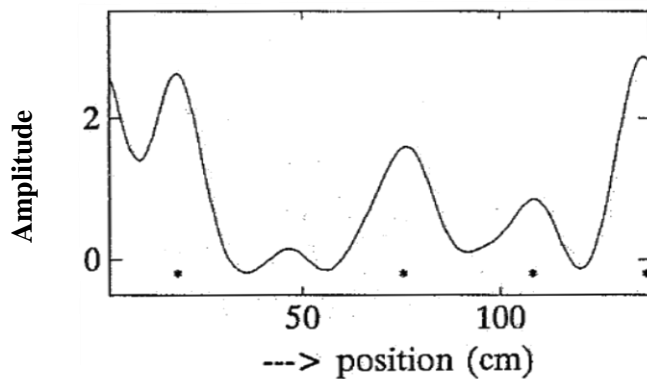


Figure 7: Transformed data using FFT of the measured data from Figure 5. (Bontsema *et al.*, 1991).

This method seems to work properly, but no weeds were present in the measured section. These weeds will lead to more peaks when transforming the spectrum. However, from a subsequent research by Bontsema *et al.* (1998) it appeared that the peaks of sugar beet plants had a higher amplitude as peaks that are present due to weeds. In this report it is also stated that the mutual distances of the sugar beet plants do not have to be exactly constant to let the FFT method work properly.

Hemming

Hemming *et al.* (2011) reported about an intrarow weeder which makes use of the method described by Bontsema. Opposed to Bontsema, this intrarow weeder makes use of image processing such that more complete information about the situation is available. With an excessive green operation, vegetation was distinguished from the soil. The binarized image indicates vegetation or soil pixels (Figure 8a). To detect the position of the crop row, all pixel values were added parallel to the row direction. A Gaussian Bell fit was used on the pixel summation to determine the centre of the crop row position (green line, Figure 8a). A search corridor with a width of two times the expected plant diameter was overlaid symmetrically with the expected row position line (white lines). In this search corridor all pixel values were summed up perpendicular to the crop row per image column. This resulted in the intensity graph in Figure 8b in which the individual crop plants can be distinguished.

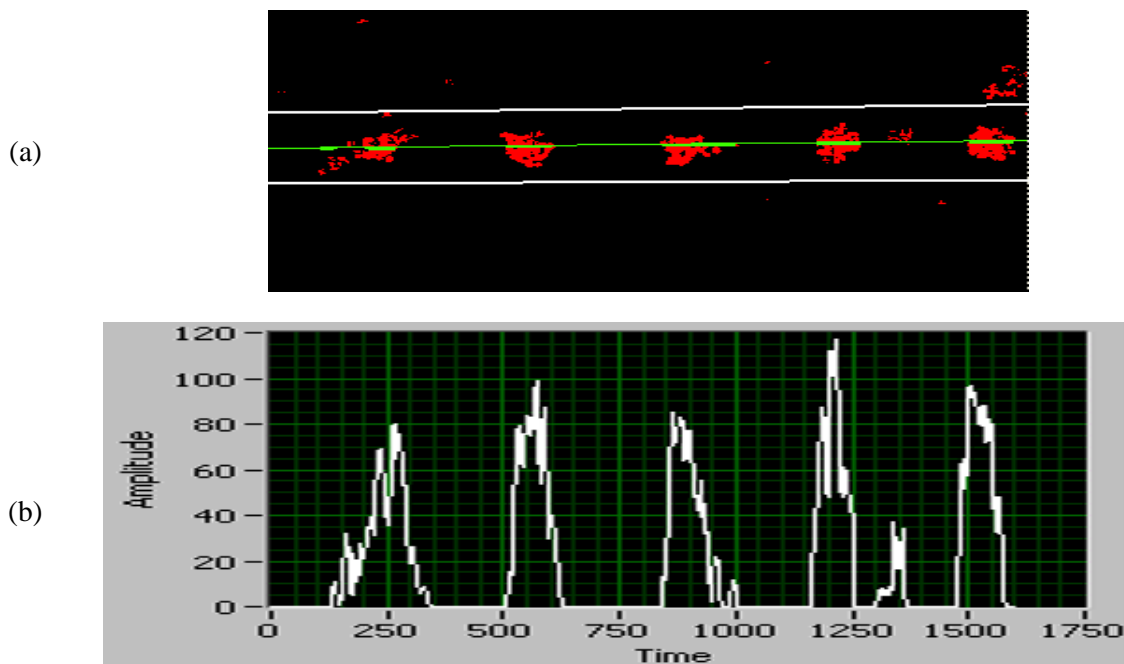


Figure 8: (a): Search corridor for the detection of plant positions in the row. Plants (red), determined row position (green centre line), border of search area (white lines). (b): associated intensity graph. (Hemming *et al.*, 2011).

Transforming the intensity graph with FFT to the frequency domain resulted in a Fourier spectrum with the contribution of the crop plants accumulated in one frequency band. Only this band was retained and transformed back to reveal the position of the crop plants. It is however not reported how this band was filtered and which band was transformed back. Also nothing was said about how this information was used to control the actuators.

Nørremark

Nørremark *et al.* (2008) reported about an intrarow weeder making use of geo-referenced crop plants. This means that at sowing of the crop, the exact position obtained by RTK-GPS was logged for each

individual seed. These exact positions were used during hoeing to avoid collision between the hoe and the crop plant. It was found that 95% of the crop plants appeared in 37.3 mm distance from its seed location. Due to GPS drift and measured deviations between seed location and plant location, a minimum RMS error of 15.6 mm can be expected in both longitudinal and latitudinal direction. Midtiby (2012) made the striking remark about this method that in the meantime between sowing and hoeing, data about the seed position can be disturbed, for instance by a pass with a tractor or, on larger scale, an earthquake, such that the actual position of the crop shifts from the logged position of the seeds. Also data can simply be lost. Both result in that hoeing with this method becomes impossible.

Midtiby

Midtiby *et al.* (2012) did research on finding the plant stem emerging point (PSEP) of a sugar beet plant in early growth stage by image processing. This was done by extracting the position and orientation of single leaves of the beet plant. PSEP estimates based on a single leaf had an average error of about 3 mm. When multiple leaves were detected per plant, the average error decreased to less than 2 mm. It has to be remarked that with this method the leaves should not overlap each other and leaves must have a regular shape.

Shrestha

Shrestha *et al.* (2004) did research on a method that compared the machine vision detected maize plant position with the manually determined position. The maize plant positions were found by summing up the pixel values in the binarized plant pixel image perpendicular to the row direction. The mean absolute error of the machine vision detection was 57 mm. This high number was mainly due to maize plants that were not found by the vision based algorithm.

Tang and Tian

Tang and Tian (2008) developed an algorithm to automatically measure maize plant spacing at early growth stages with use of image data. Plant material was separated from soil by an excessive green operation. Maize plants were differentiated from weeds by two shape parameters: area and compactness. The plant emerging point was determined by a method from Steward and Tian (1999). When compared with manual plant distance measurements, the system estimated plant spacing with an error (RMSE) of 1.7 cm or 8.3% of the mean spacing for V3 growth stage corn plants.

3 Materials and methods

3.1 Datasets

For this research datasets from Nieuwenhuizen (2009) containing images (RGB, NIR, ground truth and result images) of three adjacent rows of beet crop were available (Figure 9). Ground truth images contain human inserted information about which region in the image contains sugar beet plants, volunteer potato plants or soil. Result images contain the decision made with the algorithm of Nieuwenhuizen where to spray the glyphosate. The images contain a top view of three adjacent crop rows. Every 20 cm, the camera was triggered to make an image. This resulted in images with a size of 1628 by 202 pixels.

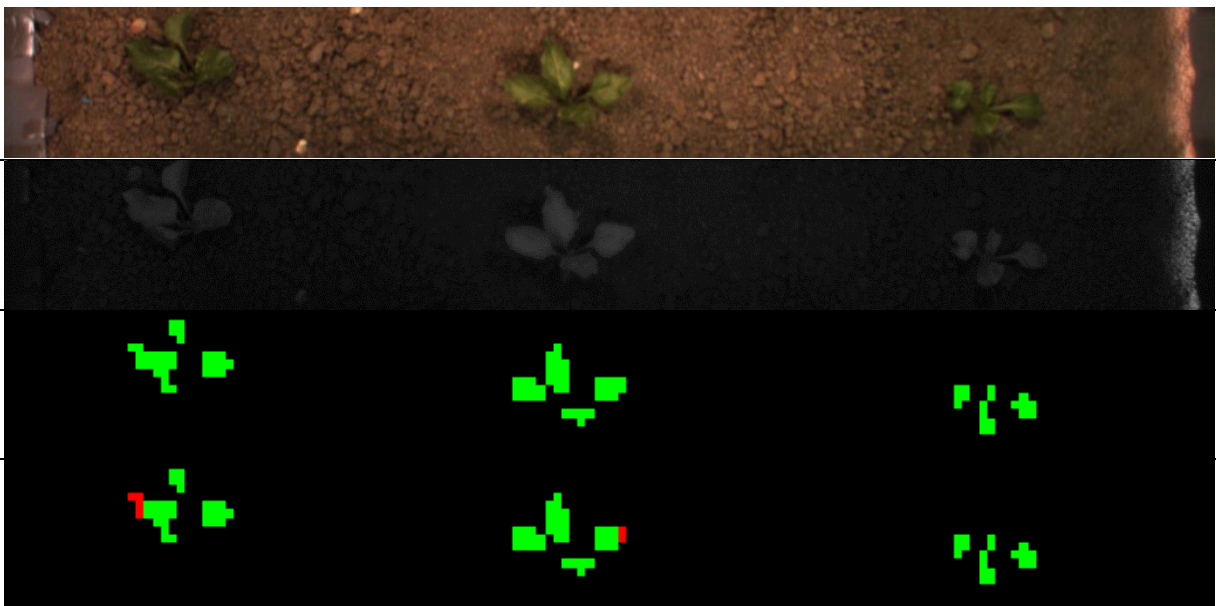


Figure 9: RGB, NIR, ground truth and result image of same region.

In Table 1 the datasets are shown that were available for this research, which are a selection of the datasets used by Nieuwenhuizen (2009).

3.2 Image processing

All image processing, calculation and programming was performed using LabVIEW (National Instruments, version 2010).

Calibration

The images could be calibrated to a metric scale using the ratio:

$$1 \text{ pixel} \Leftrightarrow 0.99 \cdot 10^{-3} \text{ meter} \quad (1)$$

This calibration was based on the length of one image in the crop row direction. According to Nieuwenhuizen one image covered a distance of 20 cm. Because the image consist of square pixels, this calibration also holds in the direction perpendicular on the crop row direction.

Merge images

Since the length of an image in the row direction corresponded with the triggering distance of the camera, adjacent images could be merged by simply connecting them on the long edge. Depending on the amount of images n , the size of the merged image becomes 1628 by $n * 202$ pixels.

Excessive green

To distinguish vegetation from soil in an image, an excessive green operation is commonly used.

$$ExG = 2G - R - B \quad (2)$$

Where R, G and B stand for the pixel colour values. This operation is first described by Woebbecke *et al.* (1995). Using a threshold makes that the image is binarized to vegetation and non-vegetation pixels. This threshold is not fixed, but depends on the circumstances of the image, like light, background colour, etc. In the article multiple formulas are examined to come up with the most suitable one to distinguish vegetation from soil pixels. It is stated in the article that the green chromatic coordinate was significantly higher for a plant than for other surfaces. Therefore the contribution of the double green pixel value relative to red and blue was used, since it raised the relative presence of green in a pixel.

3.3 Accuracy determination of plant distance

To make use of the regular plant pattern in a crop row as classification feature, it was examined how regular this pattern is in practise. Therefore plant distance histograms of two different types of datasets were made, as described below.

3.3.1 Image datasets

From two datasets originating from Nieuwenhuizen (2009) a section of consecutive RGB images was taken (Table 2). In these images the centre point of every appearing beet plant was marked as accurate as possible by hand, with use of the program Paint. These marks have the shape of red squares with a size of 8*8 pixels. The result for one image is shown in Figure 10, in which the red square dots represent the marked sugar beet centre points. Such an image was called a centre point ground truth image (CPGT image).

Table 2: Image datasets from which sections centre point ground truth (CPGT) images have been made. Second column denotes the number of images that were included in the dataset. The last three columns denote information about the content of the datasets.

Dataset	# of images	# of beet plants	# of plant distances	Distance covered [m]
2008-06-02 Clay soil	66	131	128	13.2
2008-05-28 Clay soil	100	211	208	20.0



Figure 10: Example of a centre point ground truth (CPGT) image, in which the red squares represent the marked position of the sugar beet centre point.

The CPGT images were filtered by a colour filter resulting in binarized images with only the marked beet centre points remaining. No excessive green operation was used. By obtaining the centre of mass in x- and y-direction of the red square marks, the position in terms of an x- and y-coordinate was obtained. The beet positions were collected per row using the x-coordinate (Equation (3)). This is needed since every beet row has to be handled separately.

$$\begin{cases} \text{Left row if } x < -0.25 \text{ [cm]} \\ \text{Middle row if } -0.25 \leq x \leq 0.25 \text{ [cm]} \\ \text{Right row if } x > 0.25 \text{ [cm]} \end{cases} \quad (3)$$

The plant distances were obtained by subtracting the y-coordinate of the next beet with the previous beet, such that the spacing was calculated. So from n beet positions per row, $n - 1$ plant distances could be calculated. All plant distances were collected per dataset.

3.3.2 Measurement datasets

In addition to the imaged datasets, two other datasets were used. Measurement datasets contain data about the position of a sequence of beet plants measured from a base point in the crop row. One set was obtained from the Stichting IRS. The second set was obtained from measurements in the field. The field data were measured on 29 April 2013 in a sugar beet field near Oudelande in province Zeeland. Figure 11 shows the method used to collect the positions of the beet plants. With a tape-measure the position of the centre point of each single beet plant was noted with a precision of 1 cm. The beam in the left image was placed perpendicular on the crop row to ensure a fixed base point for three adjacent crop rows that were measured. The measurements were ended just beyond ten meters from the base point. Beets were sown with a standard exterior filling precision drill.



Figure 11: Overview of measurement method to collect positions of beet plants measured from a base location in the crop row (left image). Detail of tape-measure with three beet plants, indicated by arrows (right image).

The measurement dataset from the IRS was measured on a parcel in Munnekezijl, province Friesland on 7 June 2006. This data file contains four adjacent crop rows, covering a distance of ten meters. No report was available about the measurement method, but in all probability this was equal to the above described method, since the layout of the data is equal. The complete datasets are in Appendix A.

Table 3: Overview of available measurement datasets. Columns 2 to 5 indicate qualitative information about the datasets.

Dataset	# of beet plants	# of plant distances	# of rows	Distance covered [m]
Munnekezijl	207	203	4	10.0
Oudelande	139	136	3	10.5

3.3.3 Plant distance histograms

To visualise the determined plant distances of the four datasets, histograms were made with a class width of 2.5 cm. The result is shown in Figure 12.

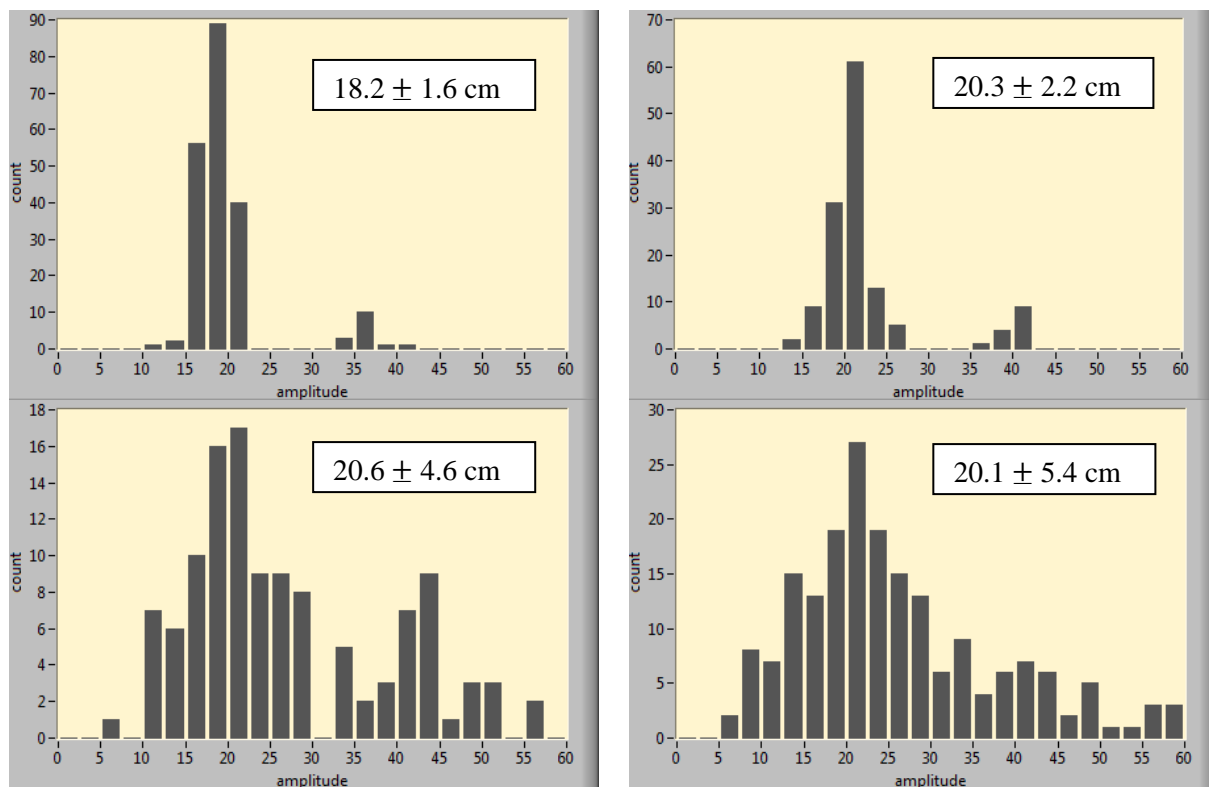


Figure 12: Plant distance histograms of datasets Munnekezijl (top left), Oudelande (top right), 2008-06-02 Clay soil (bottom left) and 2008-05-28 Clay soil (bottom right). In the text boxes the mean and standard deviation is given of the plant distance.

All histograms show a peak at the expected sowing distance. At twice the expected sowing distance a second peak is seen. This is due to missing beet plants, since the distance between the two adjacent plants is about doubled. The accuracy of the planting distance in each histogram was determined by the mean and standard deviation of the plant distances. It was assumed that plant distances in the range from 30 to 60 cm were due to missing beets, so these plant distances were halved.

From the histograms it is seen that the accuracy of the plant distance deviates a lot between the datasets. The measured datasets from Munnekezijl and Oudelande show a much more regular plant distance distribution as the image data files do. This indicates that the constant sowing pattern in the

image data files is more worse as in the measurement data files. In practise, a plant distance distribution of the measurement files is more likely than the distribution of the image data files. As indicated in the objective no extra image data files were made for this research. Therefore this research has to deal with a poorer regular pattern, which is common in all image data files available for this research (Table 1). This is probable of negative influence for the utility of the plant pattern as classification criterion as described in this report.

3.4 Linear regression method to estimate future beet positions

This chapter contains theory about linear regression and thereafter a method was introduced to use the linear regression in an online application. This method makes use of the datasets with CPGT data only, since this algorithm does not include the possibility of detecting individual beets in an image.

3.4.1 Theory

Since the sugar beet crop was sown by a precision seeder, the seed distance should be theoretically equal everywhere. From this the seeds should have a linear relationship with the row distance according to the relationship in equation (4).

$$y(n) = an + b \quad (4)$$

Where:

$y(n)$ is the position of beet number n measured from the origin [cm];

n is the beet place number. $n=0,1,2,\dots,n$;

a represents the sowing distance [cm];

b represents the modelled position of the origin [cm].

In Figure 13 a trend line was added to a series of data points that represent the position of nine beet plants with a sowing distance of 20 cm (Original data in Appendix B). This trend line was established with usage of a least squares fit and represents the linear relationship between these data points. The formula in the figure corresponds to the formula in equation (4). Besides that the position of most beet plants shows a certain deviation from its intended position, the slope of the trend line corresponds to the intended plant distance in the crop row.

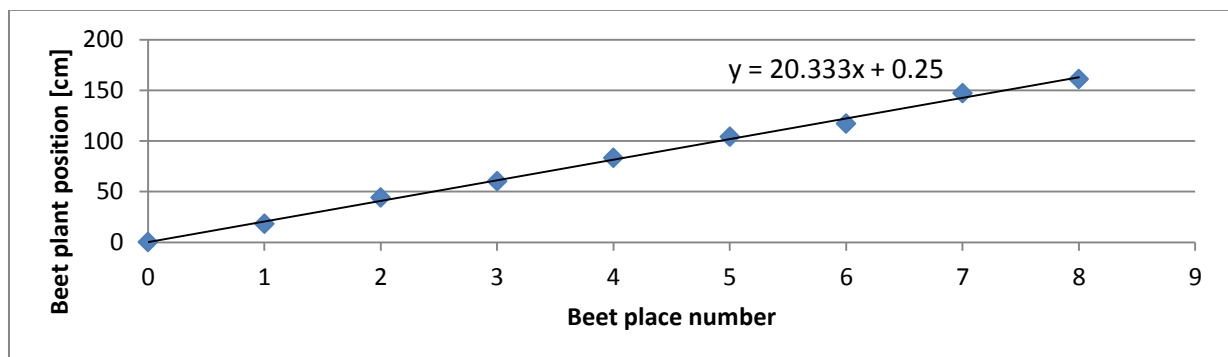


Figure 13: Model of the position of nine sugar beet plants with a sowing distance of 20 cm, with a trend line established by a least square fit.

The beet place number is related to the procedure of the seed disc in a precision seeder. The beet number is an ascending number from a decided starting point, equal to the amount of seeds that have

been sown by the precision seeder. To assign a beet number to a beet plant, the sowing distance and the starting point have to be known. These are equal to the parameters a and b from equation (4). The beet number is not automatically equal to the amount of beet plants, since missing beet plants and double germinates will occur. When a beet plant was missing, its beet number was skipped. When a double germinate occurred, both plants were having the same beet number, because both originate from the same seed. This is illustrated in Figure 14.

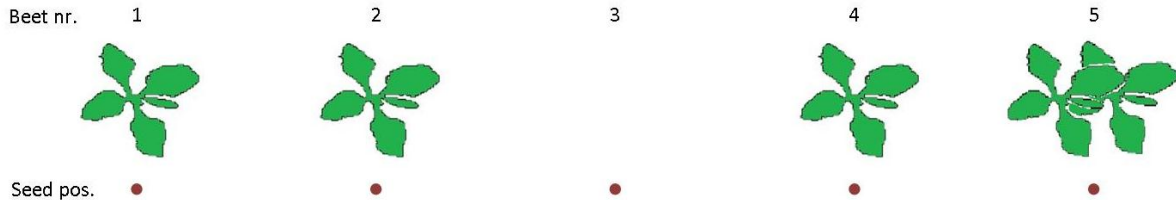


Figure 14: Image illustrating the effect of missing beet plants and double germinates on the beet number.

The linear relationship between beet number and beet position was used in the linear regression model, which determines the parameters a and b by least squares estimation to come up with the optimal linear fit. The least squares method was used, because the noise in $y(n)$ is Gaussian distributed. This was shown in the plant distance histograms in paragraph 3.3.3. By extrapolating the linear fit, the possibility exist to estimate the position of future beet plants. In the next paragraph this possibility was further investigated in an online application.

3.4.2 Linear regression method in an online application

In this section explanation will follow how to use the linear regression method in an online application.

Initial determination of sowing distance

From the research questions of this thesis it was stated that the sowing distance will be unknown on forehand. From the AgroBot requirements it was known that the classification has to be performed online, since the robot will drive in the field and has to act instantly to a passing volunteer potato plant. Since the sowing distance is needed to assign a beet number to a beet plant, it was not possible to start directly with the linear regression method. To initialize it was chosen that the first nine meters of a field were used to filter the most common plant distance, which will be a measure for the sowing distance. This nine meter row distance was relative to an expected sowing distance between 15 and 25 cm assumed to be appropriate to determine the sowing distance.

When all plant distances were determined in the initialization area, it was not possible to simply take the average of all plant distances. This is because missing plants and dual germinates will occur. Therefore a method had to be found that searches for the most frequent plant distance. For this the plant distance histogram can be used very well, since it counts the amount of times a measurement occurs in a certain range. The classes were chosen to have a width of 2.5 centimetres, equal to the histograms in paragraph 3.3.3. As after nine meters the initialization was finished, the class with the highest peak was selected and from the measurements assigned in this range the mean was calculated. This value will be the measure for the sowing distance, denoted by the parameter d [cm].

However, it was possible that when the initialization was finished, two or more peaks had the same count. This could be due to (1) the possible sowing distance was on the edge of two classes or (2) because of a large scatter of plant distances in the initialization area, no clear peak would arise. The

first problem was captured by adding a second histogram which has overlapping classes with the first histogram. In Table 4 the class borders for the first histogram and the second shifted histogram are shown.

Table 4: Calculation of class borders for the histogram and the shifted histogram. In which x is class width [cm], k is an integer on interval 0 to k_{max} representing the number of classes.

	Class lower border	Class upper border
Histogram	$k * x$	$(k + 1) * x$
Shifted histogram	$k * x + \frac{1}{2}x$	$(k + 1) * x + \frac{1}{2}x$

The second problem is solved by continuation of the initialization as long as the highest peak of one of the two histograms does not contain three or more measurements more than the second highest peak in the same histogram. This results in a longer initialization area.

In Figure 15 the two histograms are shown at the end of an initialization area of the CPGT images of dataset 2008-06-02 Clay soil. Since the highest peak in the non-shifted histogram has three more measurements than the second highest peak, the initialization stopped. So the sowing distance was in this case determined from the mean of all plant distances in the range 20 - 22.5 cm.

In the shifted histogram it is seen that the measurements were more scattered over the classes. No clear peak has raised in this histogram, so it is probable that the sowing distance was around 21.3 cm, which was on the edge of two classes in the shifted histogram.

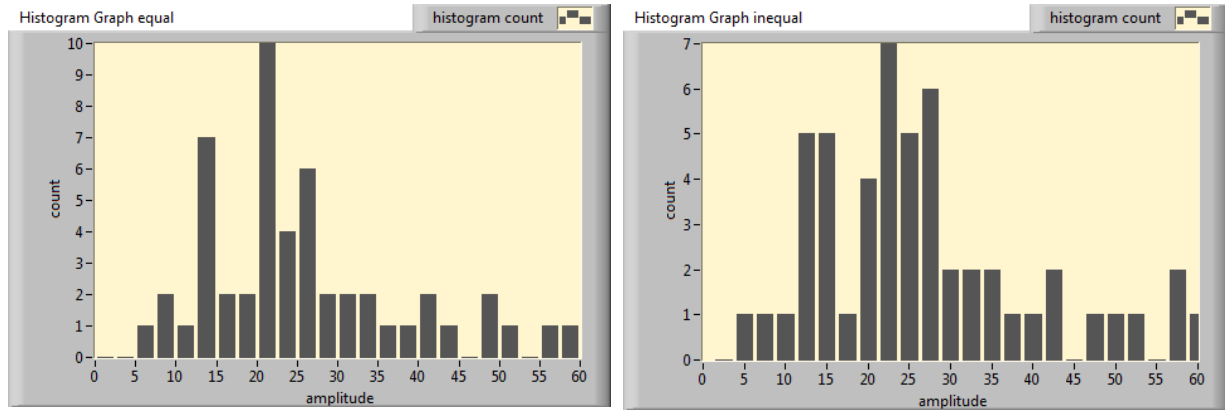


Figure 15: Non-shifted (left) and shifted histogram (right) at the end of the same initialization area. The sowing distance is determined to be in the range 20 - 22.5 cm, as it is the highest peak in the non-shifted histogram. The initialization is stopped at this moment, since the highest peak has three measurements more than the second highest peak.

Determination of next beet position

After the initialization, the estimation of the future beet positions starts. First, for each beet plant that was recognized, a beet place number was assigned. The beet number was determined by equation (5).

$$n(k) = n(k - 1) + \left[\frac{x(k) - x(k - 1)}{d} \right] \quad (5)$$

Where:

$n(k)$ is the beet number assigned to the current beet, $n(k) \in \mathbb{Z}^*$;

$n(k - 1)$ is the beet number of previous beet, $n(k - 1) \in \mathbb{Z}^*$;

$x(k)$ is the beet position [cm];

$x(k - 1)$ is the beet position of previous beet [cm];

d is the sowing distance from initialization [cm].

k is the count of detected beets, $k = 1, 2, \dots, i$;

$n(0) = 0$;

$x(0) = 0$ [cm].

The square brackets indicate that the quotient has to be rounded to the nearest integer. To be sure that the linear fit and thus the estimate of the future beet plants was representative for the current section, the nearby beets must be weighted more heavily in the linear regression function than the beets on a further distance. For now only the last ten beet plants were input for the linear regression model with the same weight. This was done to be sure that the estimate was based only on actual data and to prevent that errors from the past, that were not applicable anymore, remain in the estimation.

Because of the dispersion in beet positions it was not very accurate to determine the beet number only from the difference between the current beet position and the previous beet position. It was plausible that one of the two, or both, were out of the pattern. Therefore it was more accurate to replace $x(k - 1)$ by the estimate of it provided by the linear regression $\hat{x}(k - 1)$.

$$x(k - 1) \rightarrow \hat{x}(k - 1) \quad (6)$$

The estimated positions of the future beets in the row were calculated by extrapolating the linear regression function. The estimates of the beet position were denoted by the parameter μ .

$$\mu(n + k) = a * (n + k) + b \text{ [cm]}, k = 1, 2, \dots, i \quad (7)$$

The accuracy of the linear fit was given in terms of a mean squared error (MSE). The MSE is calculated with equation (8).

$$MSE = \frac{1}{k} \sum_{i=k-10}^k (\hat{x}_k - x_k)^2 \text{ [cm}^2\text{]} \quad (8)$$

in which \hat{x}_k represents the vector of estimated beet positions of the vector x_k with the measured beet positions in it, given by the linear regression model. The square root of the MSE represents the standard deviation.

3.4.3 Probability distribution in beet row

When the position of the future beet plants is estimated and the accuracy of the linear fit is determined, these variables have to be combined to determine from each position in the beet row the probability of presence of a beet plant. For this a Gaussian distribution function is used.

$$f(x) = e^{-\frac{(x-\mu)^2}{2\sigma^2}} \quad (9)$$

Where:

$f(x)$ is the probability of position x of presence of a sugar beet plant. $0 \leq f(x) \leq 1$;

x is the position in the beet row [cm];

$\mu(n)$ is the estimated beet position [cm];

σ is the standard deviation of the estimate μ [cm].

With this function the probability has a maximum of 1 when x is equal to μ .

The width of the distribution depends on the regularity of the plant distance in the crop row, since this is determined by the MSE (equation (8)). By setting a threshold value on $f(x)$, areas can be classified as beet location or non-beet location. With a good regular plant distance, the graph becomes smaller, indicating that the position of the next plant is predicted within a small range. Vice versa holds for a poor regular plant distance. The probability $f(x)$ can act as one of the measures to make a classification between sugar beet and volunteer potato plants.

3.4.4 Consideration about the linear regression method

At this point the further research to the linear regression method was stopped. The major problem was that an accurate determination of the individual beet position was needed. With an online method no human marked beet center points would be available, so these should be automatically detected. Tang and Tian (2008) used a method to determine the plant stem emerging point of maize plants, which was in most of the cases successful. This was because the shape and size of maize plants makes it well possible to distinguish on area and compactness. Since sugar beets have a more broadleaved shape it was assumed that this method would not work to distinguish beet plants. Although this was not proven by this research. In Midtiby *et al.* (2012) a method was explained that estimates the plant stem emerging point (PSEP) of small, non-overlapping beet plants. If at least one leaf per plant was detected, 90% of the PSEP were detected within 20 mm. Compared with the standard seeding distance of 20 cm, this would be a deviation of at maximum 10%. Nevertheless no usage was made of this method, since overlapping leaves and leaves with irregular shapes were often not detected. These leaves will be common in a sugar beet crop, especially if the crop would be more mature. Also weeds would be probably detected as sugar beets. These factors would often lead to incomplete or incorrect detections of single beet plants.

Hence a method has to be found that is based on finding a pattern in a section of the crop row, instead of putting much effort in determining the exact position of a single beet plant.

3.5 Theory of the Fast Fourier transform

3.5.1 Theory

The Fast Fourier Transformation (FFT) is a fast method to calculate the Discrete Fourier Transformation (DFT). In below section some key characteristics of the DFT were listed that were important for this research. These characteristics were derived from the book ‘ Digital image processing’ by Gonzalez and Woods (2008).

The one dimensional Fourier transform is determined by the function:

$$F(u) = \sum_{x=0}^{M-1} f(x)e^{-j2\pi(\frac{ux}{M})} \quad [-] \quad (10)$$

The inverse of equation (10) is defined as:

$$\bar{f}(x) = \frac{1}{M} \sum_{u=0}^{M-1} F(u)e^{j2\pi(\frac{ux}{M})} \quad [\text{pix}] \quad (11)$$

The Fourier (or frequency) spectrum is given by a real and imaginary part, since the Fourier Transform is a complex value:

$$|F(u)| = [R^2(u) + I^2(u)]^{\frac{1}{2}} \quad [-] \quad (12)$$

The phase angle is described as:

$$\varphi(u) = \arctan \left[\frac{I(u)}{R(u)} \right] \quad [^\circ] \quad (13)$$

Finally, the power spectrum is defined as:

$$P(u) = R^2(u) + I^2(u) \quad [-] \quad (14)$$

An extensive version of this theory can be found in Appendix G.

3.5.2 Filter mask

From a signal, discrete frequencies can be filtered out by retaining the desired frequency bands and transforming it back to the time domain, using equation (11). This operation is called inverse FFT (IFFT). A filter mask was used, in which the retained frequency bands are put to one and the omitted bands are put to zero. The filter mask was defined as a binary one dimensional array that has to be multiplied by $F(u)$. From each retained band also its symmetrical duplicate has to be kept. This means the same band number counted backwards from end of the signal. If the symmetrical duplicate is kept out, the IFFT signal has the same shape but its amplitude is half of the original. The dc term (frequency band 0) was always excluded. In Figure 16 shows how a signal with a certain frequency can be filtered out of a signal with multiple frequencies, using a filter mask that retained only band number 2 and 62.

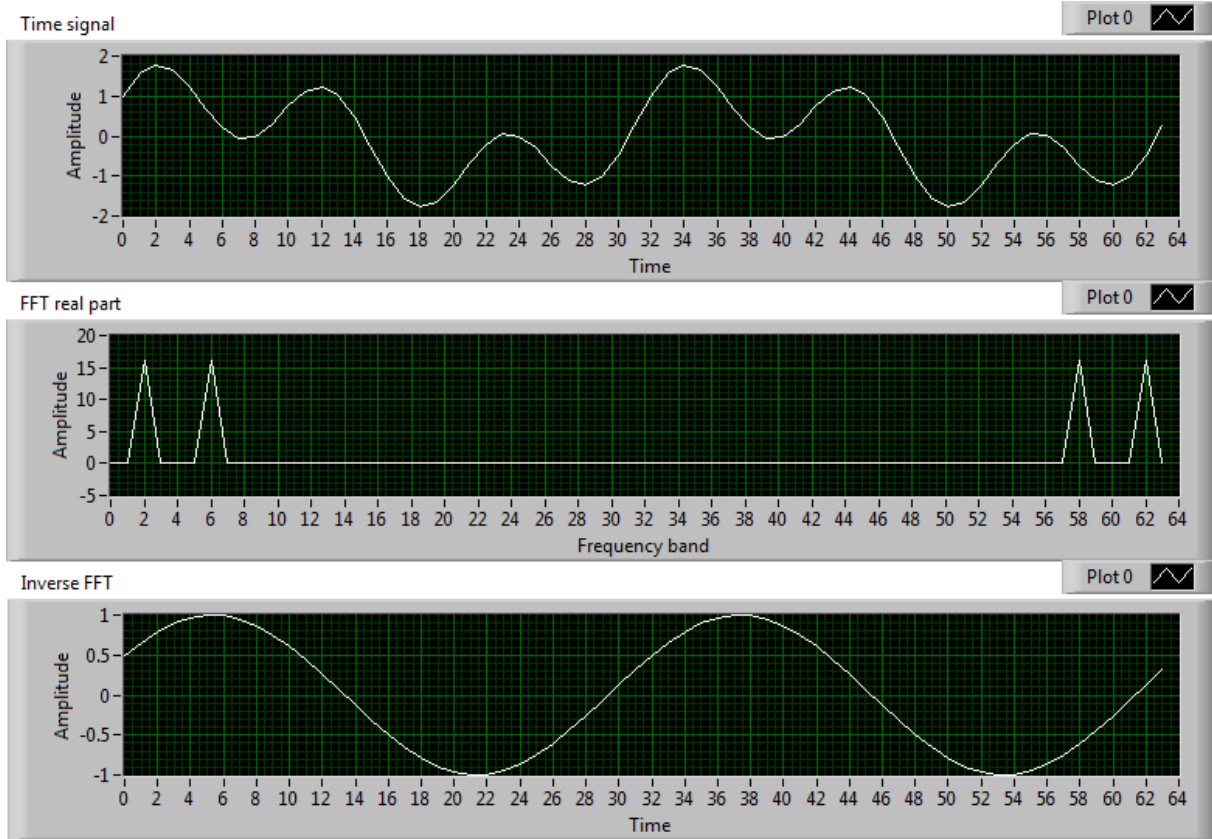


Figure 16: Example of the filter mask. A time signal $f(x)$ with two summed sine waves, the first having a frequency of 2; the second having a frequency of 6 (upper graph). This time signal was transformed to the frequency domain by FFT ($F(u)$). The real part of $F(u)$ is shown in the middle graph, resulting in peaks on frequency bands 2, 6, 58 and 62. The last two bands represent the symmetric duplicate of the first two frequency bands. The bottom graph shows the usage of a filter mask that retains bands 2 and 62, resulting in the original sine wave with frequency 2.

In case of the crop row with sugar beet plants, it was wanted to filter out the frequency band in which the beet plants appear in the signal. Which frequency band to be filtered, depends on the size of the signal and the sowing distance. Since the usage of FFT restricts that the signal has to have a size of a power of 2 (see Appendix G), it was chosen that the images have a length of 2048 pixels. Regarding the calibration (equation (1)), this image size corresponds to a crop row distance of 202.8 cm. With a standard in row sowing distance of about 20 cm about ten beet plants will appear in an image, which is decided to be enough to detect the plant pattern.

It was required that the sowing distance is not needed as a priori information. Therefore the method has to determine by itself what the sowing distance is and therefore which frequency band(s) had to be filtered out. The majority of the frequency bands provided by a Fast Fourier Transformation will not have a relation with the plant pattern of the sugar beets. As said before a standard sowing distance of sugar beets is 20 cm, such that the a number of 100,000 seeds were sown per hectare. However, in practise the seeding distance is adapted by the farmer to anticipate on conditions like an earlier sowing moment, soil conditions or weed pressure causing a changing predicted percentage of seeds that germinate (IRS, 2011). In this research a priori information was added that specifies that the sowing distance must be in the range of 15 and 25 cm. These sowing distances were translated into the frequency in which the specific sowing distance would appear in the image. This was done by dividing the image distance with the sowing distance. This resulted in a frequency of 13.5 for a sowing distance of 15 cm and 8.1 for a sowing distance of 25 cm. These frequencies are not integers. Since it is only

possible to filter out discrete frequencies, the actual frequency range was extended by increasing the maximum frequency to 14 and decreasing the lowest frequency to 8. By setting this range the frequency bands in which the pattern of the sugar beets must contribute in the image has to be searched in the range between 8 and 14. In Table 5 these discrete frequency bands are shown, with corresponding sowing distance. The symmetric duplicate of a frequency band was from here on no longer included, since it does not influence the shape of the inversed signal in the crop row direction.

Table 5: All discrete frequency bands that are present in the sowing distance range between 15 and 25 cm, with corresponding sowing distance.

Discrete frequency	Sowing distance [cm]
8	25.3
9	22.5
10	20.3
11	18.4
12	16.9
13	15.6
14	14.5

Since it is only possible to filter out a discrete frequency with the filter mask, only the sowing distances from Table 5 would be available to filter out. In practise however beets will be sown in intermediate sowing distances. Therefore the next paragraph discusses how to handle non-discrete frequencies.

3.5.3 Non-discrete frequencies

From the FFT signal bands can be retained to filter out a specific frequency from the signal. Since the Fourier transform is discrete, it is only possible to filter out discrete frequencies. If a certain frequency of interest in the signal is not discrete, it is unknown what the behaviour of the spectrum is. It might be that (1) the contribution of the non-discrete frequency is included in the two nearby discrete frequency bands or (2) that the contribution of it is spread out over a large range of discrete frequency bands. If the first case holds the problem is limited, since the two frequency bands can be filtered out and the contribution of unwanted frequencies in the inverse transformation is small. If the second case applies, this would result in a major problem, since it is unwanted to filter out a large range of frequencies. This is because it is only wanted to filter out the frequency of the beet plants. If multiple frequencies were filtered, it is likely that also noise frequencies are retained, which is unwanted.

To investigate the behaviour of non-discrete frequencies as described above, a theoretical study was performed. Therefore a sine wave was used containing 2048 samples and having an amplitude of 1. For four different frequencies (10.0; 10.2; 10.5 and 10.8) the sine wave was transformed to the frequency domain using FFT. In Figure 17 the percentage contribution of the total contribution in the range from frequency band 8 to 14 is shown. This figure only includes the real part of the spectrum. The imaginary part shows a comparable distribution.

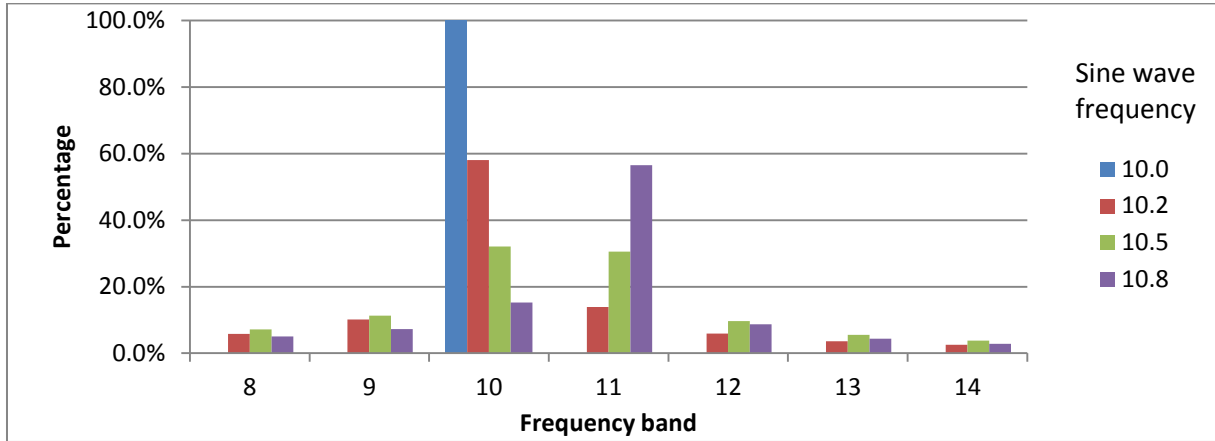


Figure 17: Percentage contribution to each frequency band per sine wave frequency of the real part of $F(u)$.

When the frequency of the sine wave was discrete, all contribution was gathered in the corresponding frequency band, as seen for a frequency of 10. With a slightly higher frequency of 10.2 only about 55% of the contribution was placed in frequency band 10. About 15% was placed in frequency band 11, the remained contribution was spread out over a range of frequency bands. With a frequency of 10.5, which is in the centre between two discrete frequencies, the contribution in frequency bands 10 and 11 was about equal. These contributions summed gave a total of somewhat more than 60%. The remained contribution was also spread out over the range of frequency bands. The sine wave frequency of 10.8 shows an equal distribution as 10.2, but symmetrically.

Since it was preferable that most of the contribution was gathered into the neighbouring discrete frequency bands, it was thought that the power spectrum $P(u)$ (equation (14)) might be useful. This was because $P(u)$ is the square from $F(u)$. Therefore it increased the larger contributions more than the smaller contributions, resulting in larger percentage contributions in the neighbouring discrete frequency bands. In Figure 18 the percentage contribution of $P(u)$ is shown for the same frequencies as in Figure 17. It is shown that more of the contribution was placed in the neighbouring discrete frequency bands.

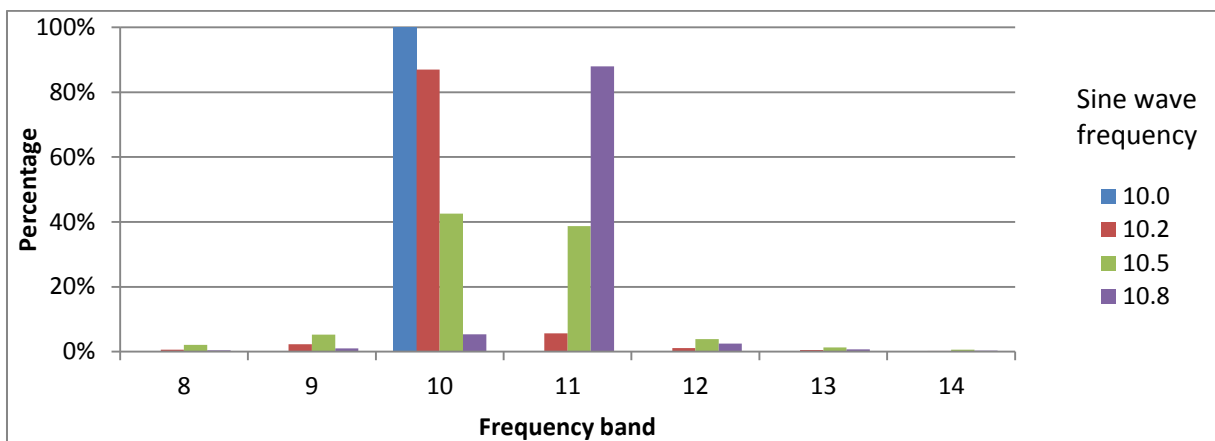


Figure 18: Percentage contribution to each frequency band per sine wave frequency of $P(u)$.

3.6 Determination of sine wave frequency and phase

FFT enhances the possibility to filter out a certain periodic signal of interest. In this paragraph a manner was found to determine the frequency and phase of this periodic signal which would correspond to the position of individual beets.

3.6.1 Simplified crop row simulation

Instead of making use of sine waves, a simplified dataset was made that resembles an intensity graph of a row of sugar beet plants. The objects in it were a simplification of the intensity graph of a sugar beet plant. In Figure 19 one triangular shaped object is shown, having a length of 70 pixels.

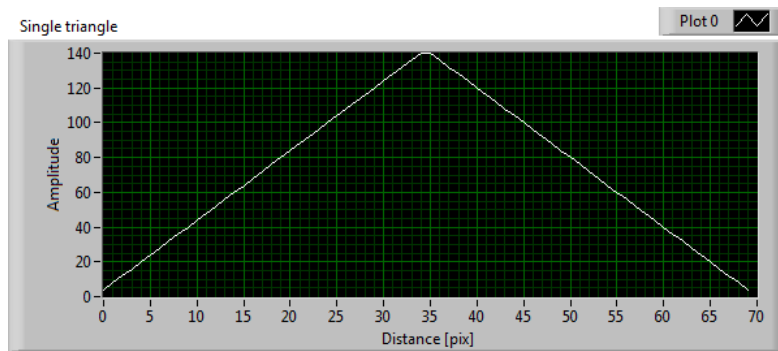


Figure 19: A single triangular shaped intensity graph, used as simplification for the intensity of an individual sugar beet plant. The distance is measured parallel over the crop row.

The simplified crop row was built up by putting multiple of these triangular shaped object on a fixed mutual pixel distance from each other. This pixel distance was measured between the peaks of the triangles. A random shift could be set on the position of the individual triangles, in order to make a crop row that is not exactly equally spaced. This provided a more realistic simplification of the crop row. Also the total simplified crop row could be horizontally shifted.

$$x_i = i * d + Rand(-1,1) * ts + hs \quad [\text{pix}] \quad (15)$$

Where:

x_i is the position of the left corner of the triangular shape [pix];

d is the mutual triangular distance [pix];

$Rand(-1,1)$ represents the uniform distributed random number in the range -1 to 1;

ts is the set point for the maximum shift of the individual triangle [pix];

hs is the horizontal shift of the total simplified crop row [pix];

i is the iteration number. $0, 1, \dots, n$;

In Figure 20 shows an example of a simplified crop after eleven iterations.

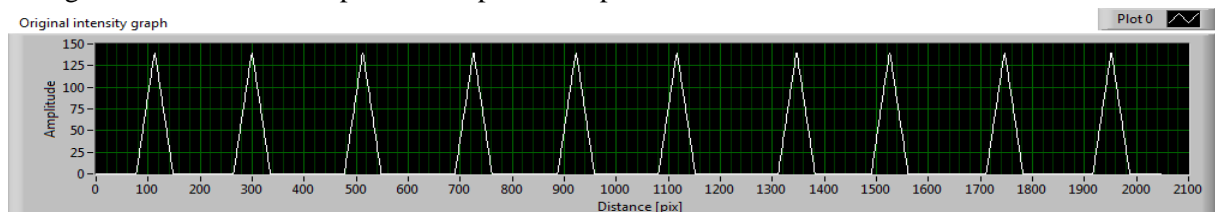


Figure 20: Intensity graph of a simplified crop row after eleven iterations, with settings $d = 204$ pix, $ts = 30$ pix and $hs = 80$ pix.

The distance variable on the horizontal axis of Figure 20 represents the distance from a certain starting point. The future crop row is located beyond the maximum distance. To use the latest information about the crop row pattern, the 2048 pixels before the maximum distance were used to determine $F(u)$.

3.6.2 Determine frequency

As from Table 5 seen, the frequency has to be detected in a demarcated range. Therefore only a demarcated range of discrete frequencies has to be considered from $F(u)$. To detect the frequency in which the objects appear in the dataset, it was needed to determine the non-discrete frequency from $F(u)$. From the theoretical part in 3.5.3 it was seen that when dealing with a non-discrete frequency, the largest part of the contribution was placed in the neighbouring discrete frequency bands. Therefore it was examined if the ratio between the amplitudes of the two discrete frequency bands is a measure for the frequency. For this the power spectrum $P(u)$ was used, since the majority of the contribution is placed in the neighbouring discrete frequency bands. Additional benefit is that $P(u)$ combines the real and imaginary part of the frequency spectrum.

From $P(u)$ the frequency band with largest amplitude was picked, which was called u_{max} . When the dataset would contain a non-discrete frequency, part of the contribution would be placed in a frequency band adjacent to u_{max} . Therefore the adjacent frequency band to u_{max} with largest amplitude was also taken out. The relative size of this amplitude to u_{max} was then calculated as the amplitude ratio (AR). An overview of the steps to calculate the amplitude ratio is given below:

1. Determine u_{max} ;
2. Determine $Side = \text{Max}\{P(u_{max} - 1), P(u_{max} + 1)\}$;
3. Calculate $AR = \frac{\text{Max}\{P(u_{max}-1), P(u_{max}+1)\}}{P(u_{max})}$.

With a sine wave with phase is 0 and an amplitude of 1, AR was calculated over the interval from frequencies between 8 and 14. This was done with a small step size of 0.001 in order to connect the amplitude ratio to the frequency. The graph in Figure 21 depicts the relationship between AR and the sine wave frequency.

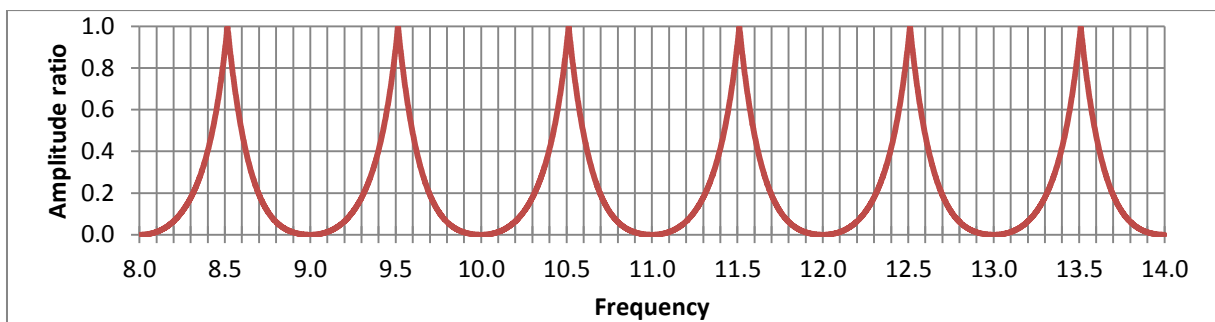


Figure 21: Amplitude ratio plotted against the sine wave frequency. This relationship was stored in a lookup table, which was used to enhance the possibility to determine the frequency at a known amplitude ratio.

The results were stored in a lookup table. This enhances the possibility to determine the frequency of a signal when AR is known. The decision trajectory for finding the frequency ($f_e =$ estimated frequency) continued from the steps above:

4. Select interval of f_i in the lookup table $\begin{cases} [u_{max} - 0.5, u_{max}] & \text{if } Side = u_{max} - 1 \\ [u_{max}, u_{max} + 0.5] & \text{if } Side = u_{max} + 1 \end{cases}$;
5. Determine f_e at the index for which holds $\min\{(AR - AR_i)^2\}$.

The steps 1 to 5 are clarified with an example in Appendix H.

3.6.3 Determine phase

After determination of the frequency, the next step was to determine the phase of the sine wave that has to be overlaid over the original intensity graph. Therefore $\varphi(u)$ from equation (13) was calculated which makes use of the real and imaginary part of $F(u)$. Since the frequency will be in most cases a non-discrete value, the phase must be calculated using the two adjacent discrete frequency bands from $F(u)$. It has been found that the ratio (ro) in which $\varphi(n)$ and $\varphi(n + 1)$ have to be included, has a linear relationship with the decimal number of the non-discrete frequency.

$$ro_{\varphi(n)} = 1 - (f_e - \lfloor f_e \rfloor) \quad (16)$$

$$ro_{\varphi(n+1)} = f_e - \lfloor f_e \rfloor \quad (17)$$

Where:

$ro_{\varphi(n)}$ is the ratio in which $\varphi(n)$ was counted;

$ro_{\varphi(n+1)}$ is the ratio in which $\varphi(n + 1)$ was counted;

$\lfloor f_e \rfloor$ is the estimated frequency rounded to integer towards minus infinity.

$$\varphi_e = ro_{\varphi(n)}\varphi(n) + ro_{\varphi(n+1)}\varphi(n + 1) \quad [^\circ] \quad (18)$$

Where:

φ_e is the estimated phase angle $[^\circ]$.

But it has been found that equation (18) has to be constrained by equations (19) and (20).

$$\varphi_n \geq \varphi_{n+1} \quad [^\circ] \quad (19)$$

$$0 < \varphi_n - \varphi_{n+1} < 360^\circ \quad [^\circ] \quad (20)$$

Since the phase is a modulo value over a range of 0 to 360°, it holds that $\varphi = \varphi + k \cdot 360^\circ$ in which k is an integer. Therefore the above constraints can always be met by adapting φ_n or φ_{n+1} .

The estimated phase angle φ_e correspond to the phase angle of a cosine wave.

In Appendix I the above findings are clarified with an example. In Figure 22 it is shown that this method was able to correctly determine the corresponding cosine wave to the original simplified crop row, because the peaks of the cosine wave do correspond to the peaks of the original signal. It has to be noticed that the amplitude of the cosine wave was irrelevant to the position of the peak, therefore it was free to choose.

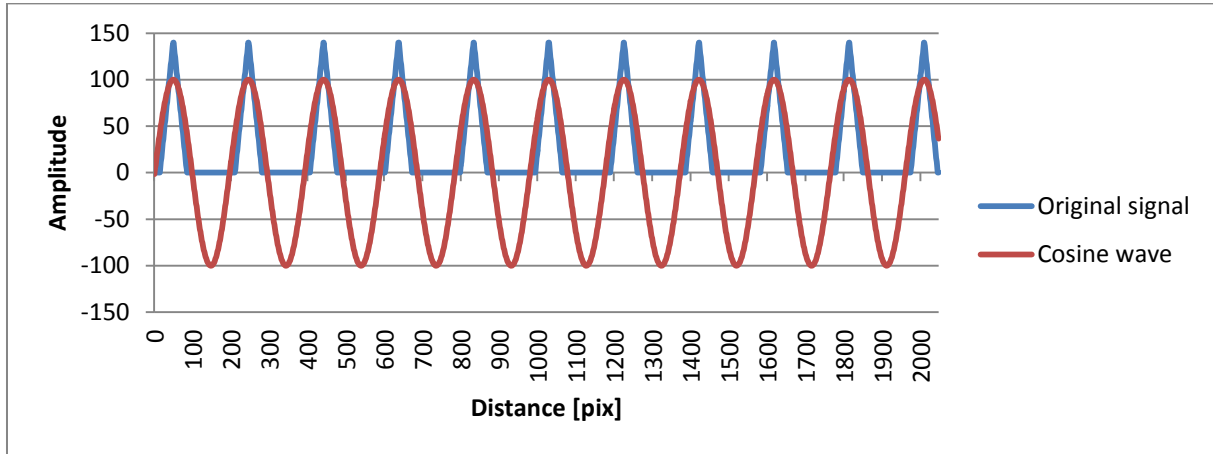


Figure 22: Original signal (blue line) for which the corresponding cosine wave was determined with use of FFT. This cosine wave having the properties frequency $f_e = 10.47$, phase angle $\varphi_e = 265.28^\circ$ and amplitude of 100 (red line).

3.7 Application of next beet position estimation method on a crop row

3.7.1 Create intensity graph

To create an intensity graph of the beet row from the image datasets, a method was used based on Hemming *et al.* (2011). This method was also used by Shrestha *et al.* (2004). In this method binarized pixel values were summed up perpendicular on the crop row. These binarized pixels were acquired with an excessive green operation on the original image. The summation was bounded by a left and right border of the row area. These borders were available from Nieuwenhuizen (2009), that made use of a Kalman filter to determine the position of the crop row in an image.

As already mentioned in paragraph 3.3.3 and as shown in Figure 12, the regular pattern in the available image datasets was rather poor. It was expected that finding the right pattern would be difficult with the method described in paragraph 3.6. Since it was desired to test the method on a more regular pattern as in practise most common occurs, the measurement datasets were used to provide a simulated crop row with a realistic plant pattern. Below it is described how a simulated crop row was build up from these datasets.

Ten individual, random, non-overlapping beet plants were selected from image dataset 2008-05-28 Clay soil. From the images of these selected beet plants, the intensity graphs were acquired.

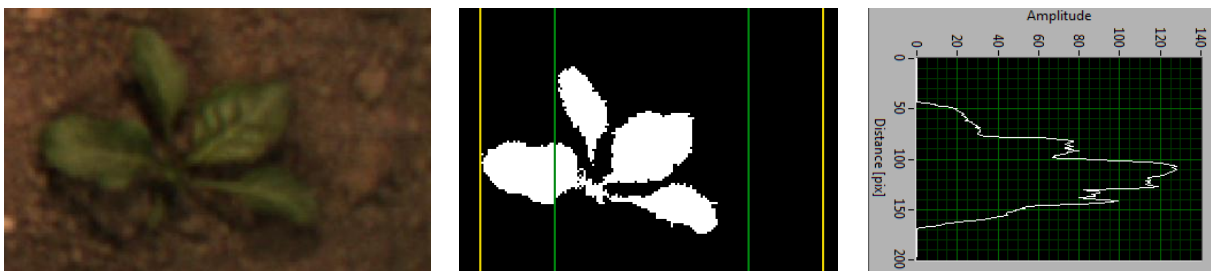


Figure 23: Original RGB image of one of the ten beets (left), binarized image resulting from an excessive green operation (middle) and intensity graph obtained a summation of the pixel values per row, bordered by the yellow lines from the binarized image (right).

These intensity graphs were used to build up a simulated crop row. The positions of the individual beets were based on the measurement datasets ‘Oudelande’ and ‘Munnekezijl’. The rows in these datasets were merged to one row. On every single beet position an intensity graph was centered, that was each time randomly chosen out of the ten available intensity graphs. With this three simulations were made for each dataset that were numbered as simulation 1 to 3.

3.7.2 Estimate next beet position

As seen in Figure 22 the ability exists to deduce the objects pattern from a simple intensity graph. This method was examined on the artificial datasets. From here on the aim was to make an estimate of the position of the upcoming beet plant. This was done by extrapolating the periodic cosine wave that corresponded to the directly underlying passed beet row. This method was named the next beet position estimate (NBPE). Equally to Nieuwenhuizen (2009) every iteration has a step size of 20 cm, indicating that the next beet position(s) were estimated over a length of 20 cm ahead. The calibration from cm to pix is equal to equation (1).

The NBPE method operates when:

$$i \geq \left\lceil \frac{FFT \text{ range}}{Step} \right\rceil \quad (21)$$

Where:

i is the iteration number (1,2,...,n);

$Step$ is the step size [pix];

$FFT \text{ range}$ is the size of the original signal [pix].

The brackets indicate that the quotient has to be rounded to infinity.

Frequency smoothing

It can be expected that the plant distance in the beet row does not change instantly. Therefore the determined frequency and phase should be interconnected between the current and prior iterations. In the determination of the current frequency, prior determined frequencies were included with a certain weight. This was called the estimated weighted frequency f_{ew} . It has to be noticed that the previous frequencies are not the frequencies determined from the weighted average, but from the previous directly determined frequencies f_e . In Table 6 two cases are described that determine the current frequency by a weighted average. The standard case was to apply smoothing. Hereby it was examined if smoothing provides a more accurate NBPE.

Table 6: Two cases describing the weight of current and prior determined frequencies (f_i) in the determination of the current frequency with a weighted average.

Iteration	Weight of f_i					
	i	$i - 1$	$i - 2$	$i - 3$	$i - 4$	$i - 5$
With smoothing	0.2	0.2	0.1	0.1	0.05	0.05
Without smoothing	1	0	0	0	0	0

Phase smoothing

Smoothing the phase angle cannot be done equally as the frequency with a weighted average. This is because the phase does depend on the frequency and is hence different at each iteration. Therefore

only a check was invented that compares the outgoing phase after one step of the previous iteration, with the ingoing phase of the current iteration (Figure 24). With exactly interconnected consecutive cosine waves these phase angles will be equal to each other. So a smaller (absolute) difference indicates a larger agreement between the consecutive cosine waves.

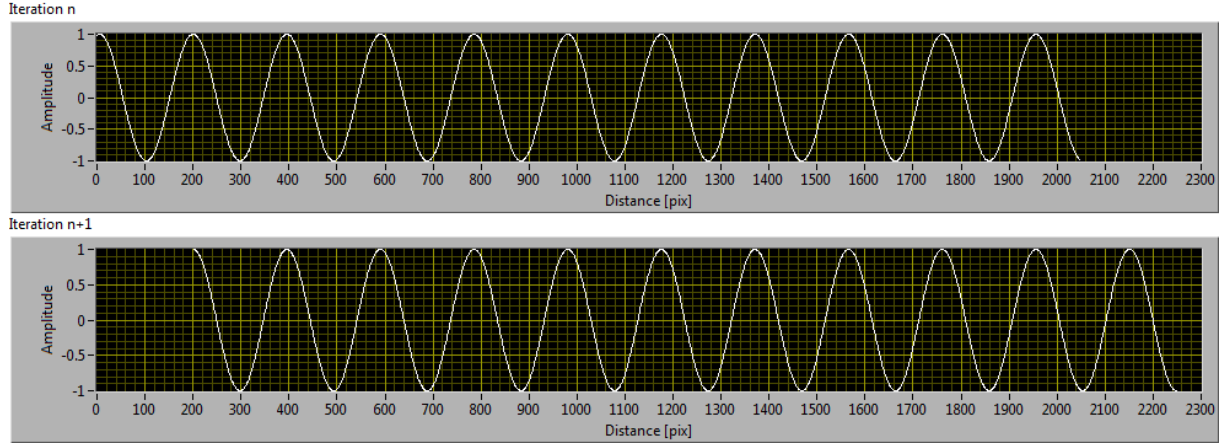


Figure 24: Two cosine waves belonging to subsequent iterations having a frequency of 10.5 and an amplitude of 1. To be interconnected, the (ingoing) phase of the current cosine wave should be equal to the outgoing phase of the previous cosine wave after one step. The step size in this example was 202 pix.

This indicator has not been used further, because it was unknown how to use it and whether it was justified to adjust the determined phase in the current iteration with the previous iteration.

Probability distribution

In Figure 25, a random iteration of a simulation is shown. It is seen that the cosine wave fits on the intensity graph and was extended with one step that serves the next beet position estimate.

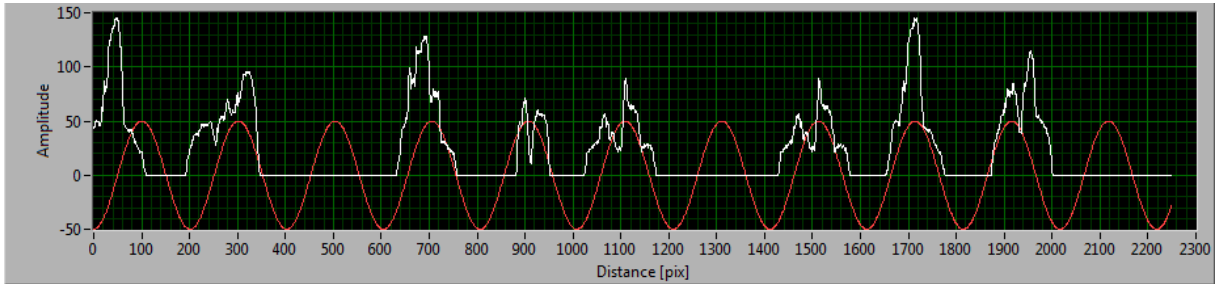


Figure 25: Original signal in the range from 0-2048 pix (white line) and associated cosine wave (red line), which was extended by one step to represent the future beet position estimate. The amplitude of the cosine wave was increased to 50 for better visibility.

For the next beet position estimate a probability distribution has to be made that represents the estimated probability of the position of the sugar beet plant in the next step. This could have been done on several manners like a normal distribution or a simple triangle shape. But for now the positive part of the cosine wave was taken, with an amplitude of one causing a probability ranging from 0 to 1. The probability distribution (P) of the next beet position estimate from Figure 25 is shown in Figure 26. From this it can be extracted that the centre point of the next beet plant would be most probably positioned on 2291 pix.

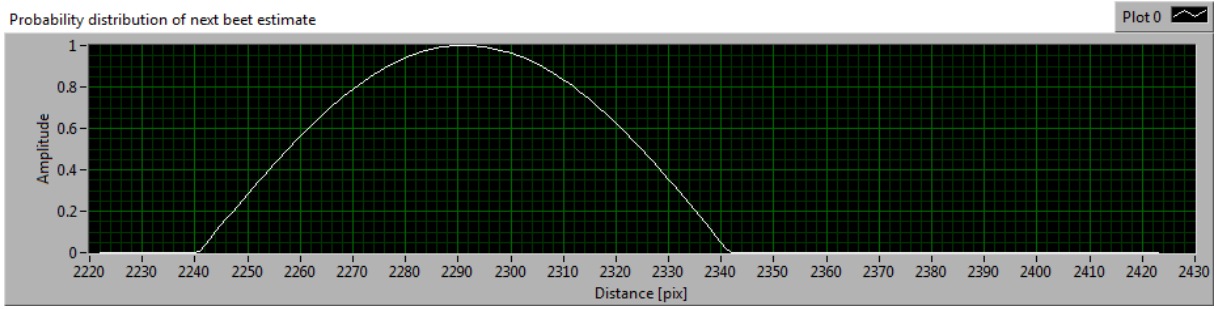


Figure 26: Probability distribution P of the next beet position estimate from Figure 25, using the positive part of the cosine wave with an amplitude of 1.

3.7.3 Accuracy determination

Two different measures were performed to determine the accuracy of the NBPE method. The first was based on the difference between the position of the peak of the probability distribution ($x_{P_{max}}$) and the beet position (x_{bp}). These beet positions were known from the measured beet positions in the measurement datasets and the determined beet positions in the CPGT image datasets. For every beet position ε [pix] was determined, which was obtained by the following steps:

1. Determine the search area by $0.5 \cdot \frac{FFT \text{ range}}{f_{ew}}$;
2. Centre the search area over x_{bp} ;
3. Determine $x_{P_{max}}$ from the search area;
4. $x_{P_{max}}$ is accepted if $P_{max} \geq 0.9$, otherwise this beet position was classified as not found;
5. $\varepsilon = x_{P_{max}} - x_{bp}$, if $x_{P_{max}}$ was accepted.

To limit the search area by half of the (determined) plant distance (step 1), it was ensured that the probability distribution corresponds to the particular beet. This value of 0.5 was chosen to be adequate. The determination of ε is further clarified with Figure 27.

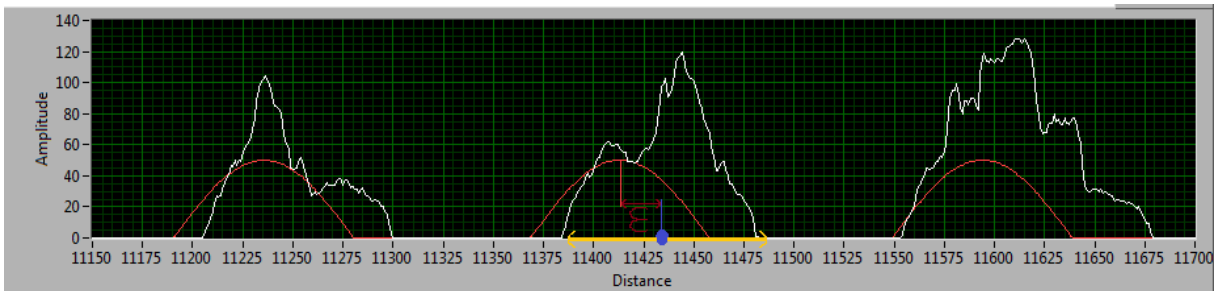


Figure 27: Explanation of the determination of ε for the middle beet. A search area (yellow line) as wide as half the determined plant distance was centered over the beet position x_{bp} (blue dot). In this area the maximum of the probability distribution has to be taken. If $P_{max} \geq 0.9$, ε was determined as $x_{P_{max}} - x_{bp}$.

The numbers of found and non-found beets were summed up. From ε the mean and standard deviation were determined. ε was calibrated from pix to cm by equation (1), allowing to determine the accuracy of the next beet position estimate in a metric unit.

The second accuracy measure was based on the probability P at the beet position x_{bp} , which was called P_{bp} . The determination of this measure is clarified in Figure 28. P_{bp} is plotted against the beet

position, allowing to explore the performance of the next beet position estimate over the simulated crop row. The row distance variable was calibrated to a metric scale.

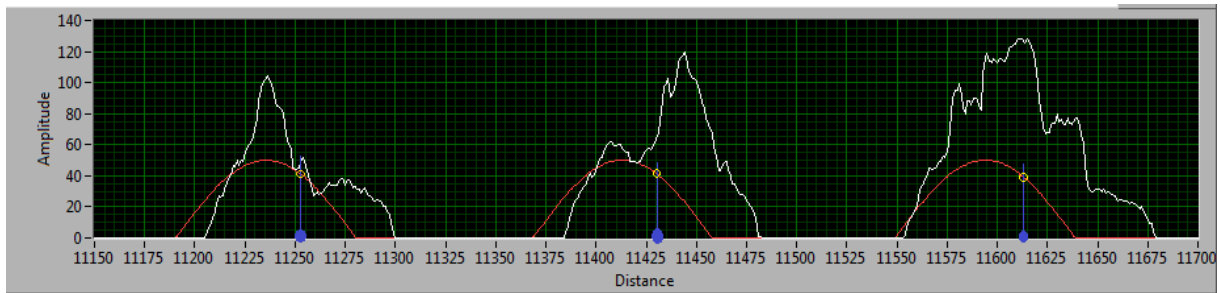


Figure 28: Explanation of the determination of P_{bp} . At the beet position x_{bp} (blue dot) P was determined (intersects in yellow circle) for every particular beet.

3.7.4 Effect of missing beet plants

Since in a normal beet row often missing beet plants will occur, it was examined how these missing beet plants do influence the quality of the NBPE. A random section was taken from one of the simulations, that did not contain a missing beet. The next beet position estimate of this section was determined and it was decided that this matched the true beet position. So $\varepsilon = 0$ cm and $P_{bp} = 1.0$. This next beet position estimate was determined for this signal separately, so without frequency smoothing. Subsequently the next beet position was estimated whereby in every iteration one individual beet was randomly deleted, until one beet was left. At every iteration the next beet position estimate was determined and from comparison with the base situation ε and P_{bp} were calculated. This method was repeated 500 times, in order to examine multiple different sequences of beet plants.

3.7.5 Effect of volunteer potato plant

The behaviour of the NBPE method was checked when a volunteer potato is present in the crop row. A random volunteer potato was taken from an image dataset. This potato with corresponding intensity graph is shown in Figure 29.

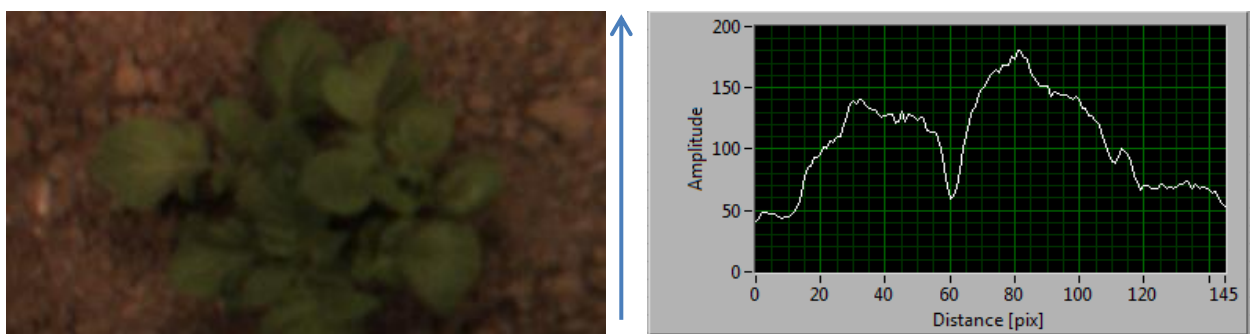


Figure 29: Volunteer potato with corresponding intensity graph. Arrow indicates the direction of the distance variable in the intensity graph.

A random iteration of one of the simulations was taken that served as base. For this part the next beet position estimate was determined without frequency smoothing, which served to compare with the signals with volunteer potato in it. These were created by inserting the intensity graph of the volunteer potato at a random position to the existing intensity graph. It was assumed that a volunteer potato in the crop row overgrows the present beets, so no beets were seen in the intensity graph at the position of the volunteer potato. With the above described methods P_{bp} and ε were determined and compared with the base situation. To have sufficient samples, 500 iterations were performed.

4 Results

4.1 Image datasets

In Figure 30 and Figure 31 two examples are shown of a section of the intensity graph of an image dataset. The corresponding cosine wave determined by the algorithm is shown, as well as the intensity graph of the next step. In Appendix C multiple examples are shown.

Figure 30 shows a section of an intensity graph of an image dataset having a proper regular plant pattern. It can be seen that this pattern was detected reasonably correctly, since the determined cosine wave corresponds to original signal. Contrary Figure 31 shows a section of an intensity graph from which the determined cosine wave corresponds less well to the original signal.

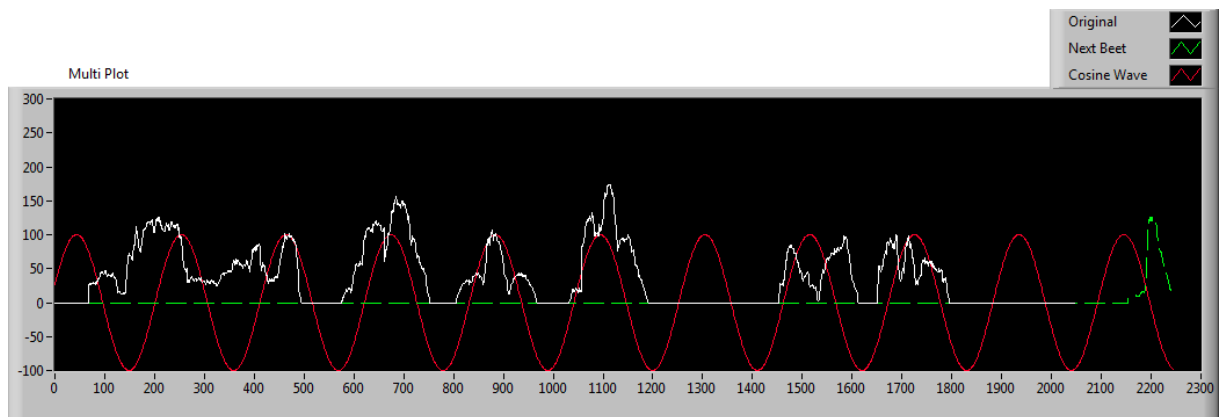


Figure 30: Random original signal from dataset 2008-05-28 Clay Soil (white line), corresponding cosine wave with properties $f_e = 9.74$ and $\varphi_e = 15^\circ$ (red line) and next iteration intensity graph (green line).

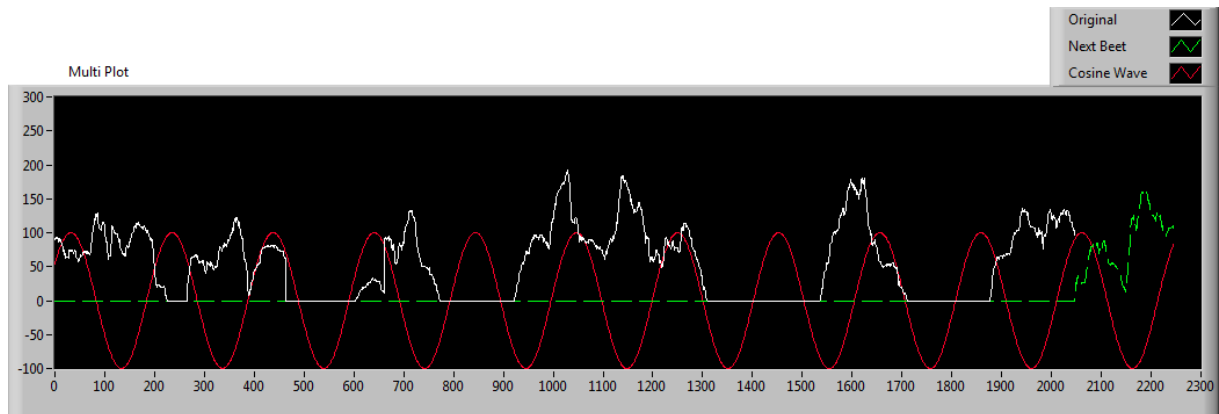


Figure 31: Random original signal from dataset 2008-05-28 Sand Soil (white line), corresponding cosine wave with properties $f_e = 10.09$ and $\varphi_e = 33^\circ$ (red line) and actual next iteration intensity graph (green line).

4.2 Metric accuracy

In Table 7 the results are shown that determine the accuracy of the NBPE for the simulations of the datasets 'Oudelande' and 'Munnekezijl'. Also the percentage of found and non-found beetles were provided to enable mutual comparison between the simulations and datasets. It should be noted that

the nine beets from the initialization area that were never been found, were not included in the non-found beets.

Table 7: Results with frequency smoothing (Table 6), indicating the number of beet plants found and not found by the algorithm per simulation of datasets ‘Oudelande’ and ‘Munnekezijl’. From the found beets, the mean and standard deviation of ε were determined.

Simulation	# of found beets (% of total)	# of non-found beets (% of total)	ε mean [cm]	ε standard deviation [cm]
Oudelande 1	124 (97)	4 (3)	-0.5	2.7
Oudelande 2	126 (98)	2 (2)	-0.3	2.5
Oudelande 3	124 (97)	4 (3)	-0.3	2.5
Munnekezijl 1	187 (96)	8 (4)	0.4	2.3
Munnekezijl 2	184 (94)	11 (6)	0.6	2.2
Munnekezijl 3	185 (95)	10 (5)	0.9	2.1

Table 8 shows the results without frequency smoothing (Table 6). A two sided independent T-Test has found no significant difference between the case with frequency smoothing and the case without frequency smoothing. The outcomes of the T-Tests are shown in Appendix D.

Table 8: Same as Table 7, but without frequency smoothing (Table 6).

Simulation	# of found beets (% of total)	# of non-found beets (% of total)	ε mean [cm]	ε standard deviation [cm]
Oudelande 1	125 (98)	3 (2)	-0.6	2.8
Oudelande 2	126 (98)	2 (2)	-0.3	2.8
Oudelande 3	128 (100)	0 (0)	-0.2	2.9
Munnekezijl 1	182 (93)	13 (7)	0.5	2.4
Munnekezijl 2	186 (95)	9 (5)	0.8	2.4
Munnekezijl 3	186 (95)	9 (5)	0.9	2.1

The performance of the NBPE was also tested on the image datasets with CPGT (Table 2). The results are shown per crop row in Table 9 and Table 10. Only the case with frequency smoothing was tested, since no difference was expected regarding the previous results.

Table 9: Results for image dataset 2008-05-28 Clay Soil, with frequency smoothing

Simulation	# of found beets (% of total)	# of non-found beets (% of total)	ε mean [cm]	ε standard deviation [cm]
Left Row	45 (61)	29 (39)	-0.3	3.7
Middle Row	51 (71)	21 (29)	0.1	3.7
Right Row	52 (78)	15 (22)	0.3	3.7

Table 10: Results for image dataset 2008-06-02 Clay Soil, with frequency smoothing

Simulation	# of found beets (% of total)	# of non-found beets (% of total)	ε mean [cm]	ε standard deviation [cm]
Left Row	29 (67)	14 (33)	0.2	3.9
Middle Row	32 (74)	11 (26)	0.8	3.1
Right Row	31 (72)	12 (28)	-1.2	4.0

4.3 Accuracy determination over the crop row

In Figure 32 the results for simulation 1 of dataset ‘Oudelande’ are shown. Simulations 2 and 3 are in Appendix E. In these graphs all beet positions are plotted against their determined probability P . On the horizontal axis it can be seen that the length of the dataset is just over 3000 cm. Every single beet position is represented by a blue dot. The larger P is, the better the particular beet position was estimated. Because all three simulations were based on the same dataset, the positions of all dots on the horizontal axis are equal.

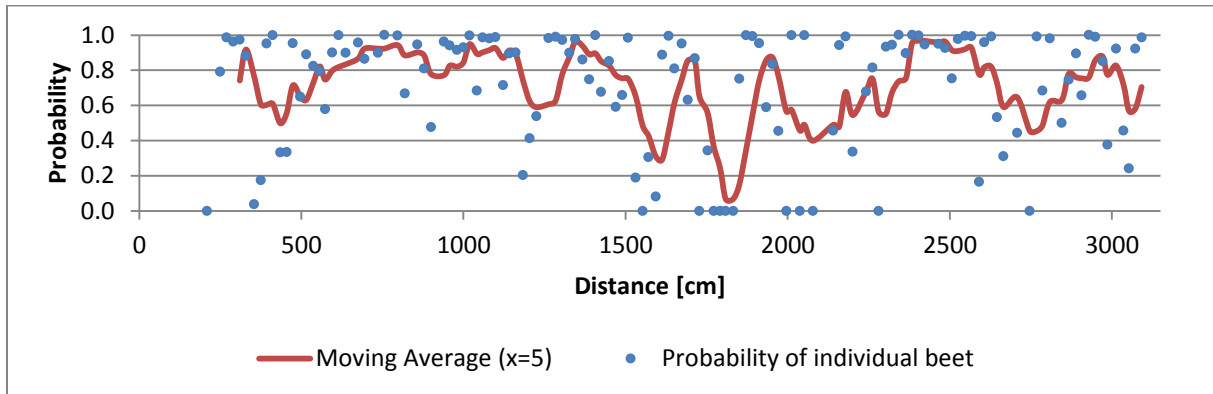


Figure 32: Determined probabilities P by the next beet estimation at the beet positions x_{bp} from dataset ‘Oudelande’ for simulation 1 (blue points). Red line represents the moving average of P with $x = 5$.

A striking observation is in the interval roughly between 1600 and 1800 cm. In simulation 1 some beet positions in this interval were badly estimated, regarding the two valleys in the moving average line. In simulations 2 and 3 these valleys were not seen at all.

In Figure 33 the result is shown for simulation 1 of dataset ‘Munnekezijl’. Simulations 2 and 3 are shown in Appendix E.

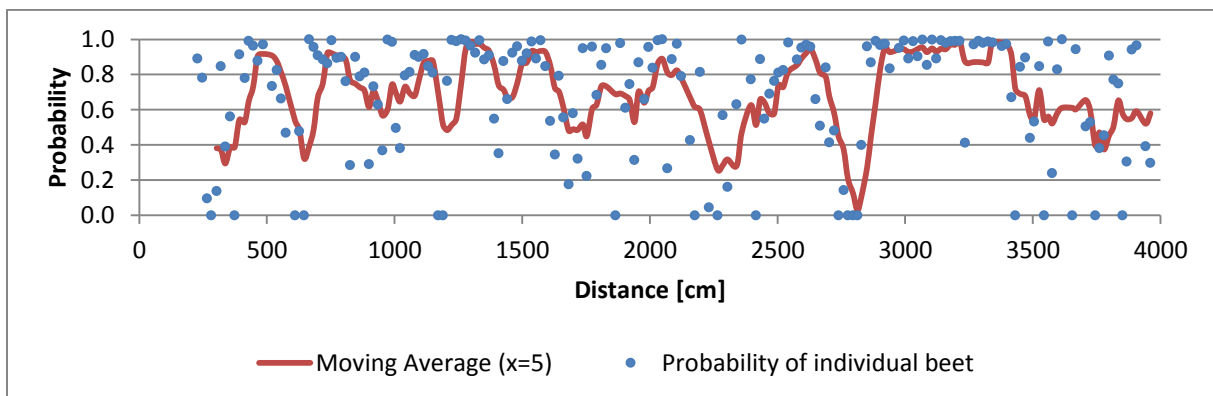


Figure 33: Determined probabilities P by the next beet estimation at the beet positions x_{bp} from dataset ‘Munnekezijl’ for simulation 1 (blue points). Red line represents the moving average of P with $x = 5$.

Similar to the simulations of dataset ‘Oudelande’, also in these simulations differences can be seen at the same locations. For instance around 2100 pix in simulation 2 a valley is seen, contrary to simulations 1 and 3 where the moving average remained high. On the other hand, at about 2800 pix all simulations show a valley, possibly indicating that some beets in this region will not be in the pattern.

Also for the image datasets with CPGT the probabilities P at the beet positions x_{bp} were determined. In Figure 34 and Figure 35 both the left row is shown for the two datasets. The middle and right rows of both datasets are shown in Appendix E.

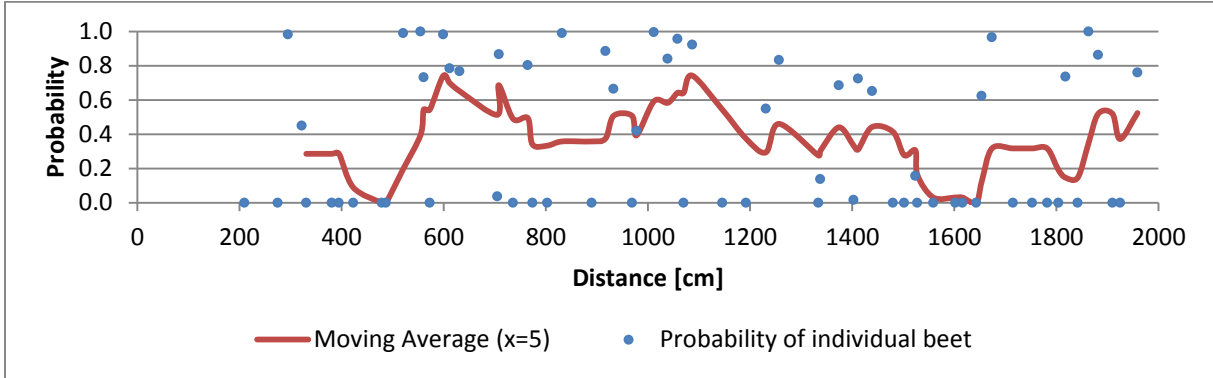


Figure 34: Determined probabilities P by the next beet estimation at the beet positions x_{bp} from dataset ‘2008-05-28 Clay Soil’ for the left row (blue points). Red line represents the moving average of P with $x = 5$.

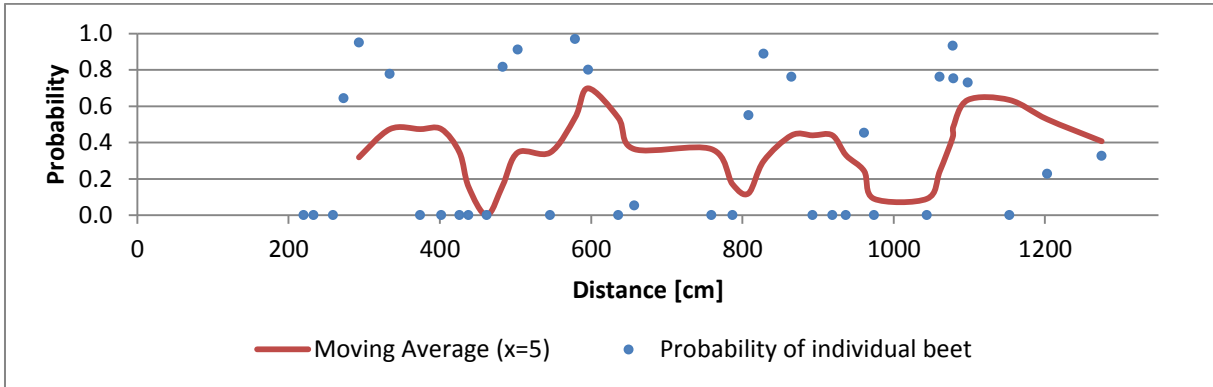


Figure 35: Determined probabilities P by the next beet estimation at the beet positions x_{bp} from dataset ‘2008-06-02 Clay Soil’ for the left row (blue points). Red line represents the moving average of P with $x = 5$.

4.4 Effect of missing beet plants

In Figure 36 the base signal without missing beet plants is shown, originating from dataset ‘Oudelande’ simulation 3. The next beet in this signal was estimated on position 5023 pix. Two striking signals were taken out. In Figure 37 a signal is shown containing only four beets, but with a reasonable correct next beet position estimate. In Figure 38 an example of a signal is shown having three missing beet plants, in which the next beet position was estimated incorrect.

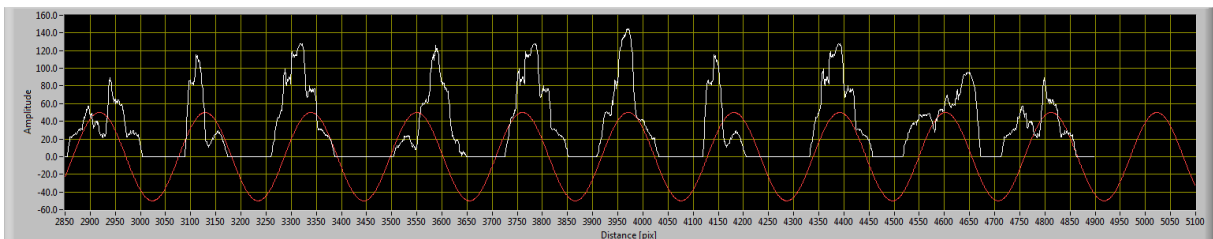


Figure 36: Base signal without missing beet plants originating from dataset ‘Oudelande’ simulation 3, in the range 2850 to 4898 pix. Next beet was estimated at 5023 pix.

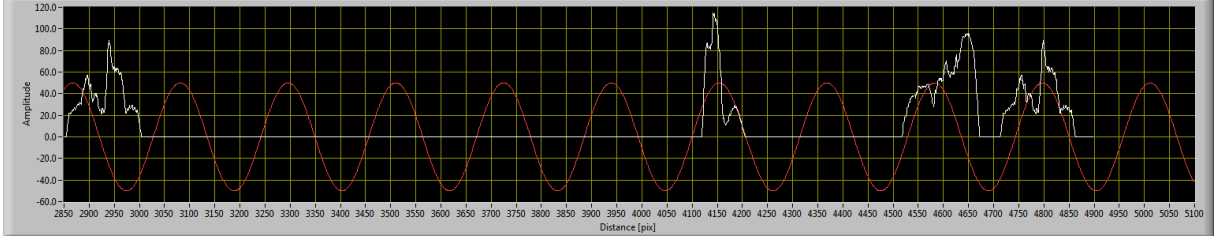


Figure 37: Iteration containing only four beets, but with an accurate estimation of the next beet position.

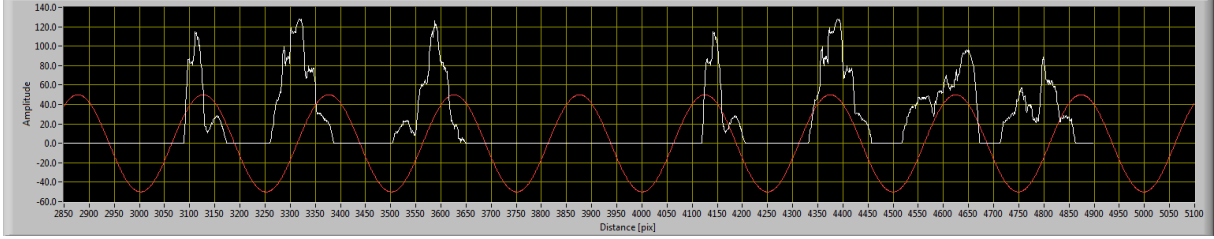


Figure 38: Iteration containing seven beets, but with a false estimation of the next beet position.

Table 11 shows the results of 500 simulations with missing beet plants. These results are presented as the mean and standard deviation of ε , per number of beets left in the intensity graph. Next to this the number and percentage of found beets are given, since ε was only determined from these found beets. The table also shows the count and percentage within the bounded ranges of $|\varepsilon| \leq 3$ cm and $P_{bp} \geq 0.7$. It is seen that the two measures often show equal counts. This can be ascribed to change, because it was a coincidence that at this particular frequency an offset of 3 cm from the peak of the cosine wave corresponded to a probability of 0.7. In the cases with less beets left the counts correspond less often, because the frequencies could be determined less accurate.

Table 11: Accuracy results of missing beet plants in the intensity graph. Results were presented per number beets left from the base intensity graph of Figure 36. The first two columns show the mean and standard deviation of ε , together with the number and percentage of found beets. In the columns beside the count and percentage within the bounded ranges of $|\varepsilon|$ and P_{bp} were given.

# of beets left	ε mean [cm]	ε st. dev. [cm]	# of found beets (% of total)	Count $ \varepsilon \leq 3$ cm (% of total)	Count $P_{bp} \geq 0.7$ (% of total)
10	0.0	0.0	500 (100)	500 (100)	500 (100)
9	-0.5	1.7	500 (100)	453 (91)	453 (91)
8	-0.3	1.6	430 (86)	373 (75)	373 (75)
7	-0.3	2.0	424 (85)	331 (66)	329 (66)
6	0.0	2.4	408 (82)	265 (53)	263 (53)
5	0.4	2.4	399 (80)	249 (50)	247 (49)
4	0.5	2.8	360 (72)	197 (40)	215 (43)
3	0.7	2.8	299 (60)	197 (40)	194 (40)
2	0.4	2.5	250 (50)	212 (42)	180 (36)
1	-0.5	2.0	259 (52)	216 (43)	216 (43)

4.5 Effect of volunteer potato plant

In Figure 39 the base signal is shown, originating from dataset ‘Oudelande’ simulation 2. In Figure 40 a random example is shown where the intensity graph of the volunteer potato is added. It can be noticed that the cosine waves of Figure 39 and Figure 40 do still correspond to each other and the next beet position estimate was little influenced by the presence of the volunteer potato in the intensity graph. Contrary Figure 41 shows an example of an iteration in which the presence of the volunteer potato caused a false next beet position estimation.

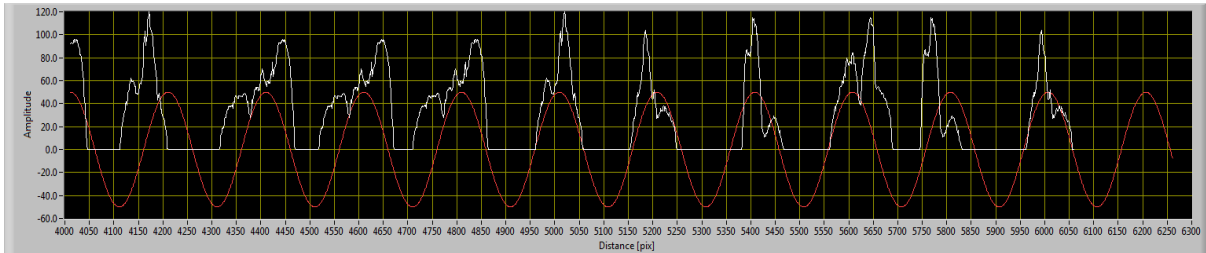


Figure 39: Base signal (white line) without volunteer potato originating from dataset ‘Oudelande’ simulation 2, in the range 4012 to 6059 pix. Next beet was estimated at 6206 pix.

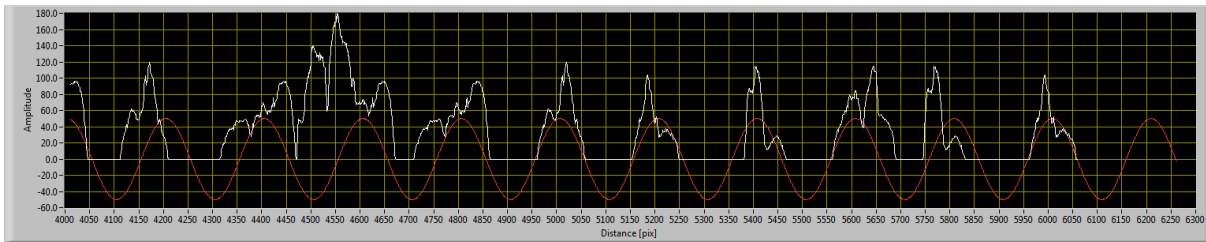


Figure 40: Random iteration with an accurate estimation of the next beet position, despite the presence of a volunteer potato in the intensity graph.

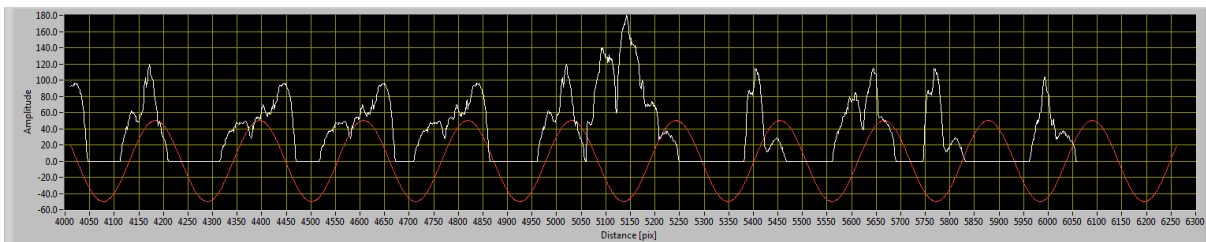


Figure 41: Random iteration with a false estimation of the next beet position, due to the presence of a volunteer potato in the intensity graph.

In Table 12 the results for ε and P_{bp} are shown. These results are presented as the count within a given range of the parameter. From this count the percentage of the total was calculated. In Appendix F the original data is shown. The accuracy for ε was -0.1 ± 1.35 cm, but it has to be noticed that this was only determined from the found beets. 370 of the 500 next beet positions were determined to be found.

Table 12: Count within the bounded ranges of the absolute value of ε and P_{bp} for 500 iterations with a volunteer potato in the intensity graph. The percentage was determined by dividing the count with the amount of iterations.

$ \varepsilon $ [cm]	Count	% of total
≤ 0.5	158	32
≤ 1.0	238	48
≤ 1.5	281	56
≤ 2.0	316	63
≤ 2.5	336	67
≤ 3.0	357	71

P_{bp}	Count	% of total
≥ 0.9	235	47
≥ 0.8	300	60
≥ 0.7	340	68
≥ 0.6	359	72
≥ 0.5	365	73

5 Discussion

The method of estimating the position of the future crop plant with use of the determined crop pattern of the foregoing area is a method where no explicit research had been done to yet. Therefore it is hard to compare the results of this research with results of others. Other research in this segment was mainly based on the determination of the exact plant position, instead of using the overall plant pattern to estimate the position of a single plant.

5.1 Literature

The objective for Bontsema *et al.* (1991) to use FFT on a crop row signal differs from the objective for this research. Bontsema was interested in revealing the exact positions of the crop plants, while this research focusses on determining the correct pattern of the crop plants. The disadvantage of Bontsema's method is that the crop plants had to be much larger than the other plants, otherwise these other plants were also detected as crop plants.

It was expected that also Hemming *et al.* (2011) was interested in revealing the exact crop plant positions like Bontsema did. Unfortunately no exact information was provided about detection of these crop plants and about the discrimination of the weed plants.

5.2 Materials and methods

Datasets

Because of a poor regular pattern in the image datasets it was needed to create simulated crop rows to test the algorithm on. The hand measured plant distances in a real sugar beet field made that these simulated datasets match a real beet row with missing beet plants at a growth stage just before leaf overlap. A disadvantage of the simulated crop rows was that it was always assumed that the position of the leaf area center corresponds to the plant stem emerging point. This made that the intensity graphs were in fact more regular. Another disadvantage of the simulated crop rows was that these contain no irregularities like (parts of) volunteer potatoes or weeds, opposed to the image datasets.

Fast Fourier transform

To detect the pattern of the beet plants in a row of sugar beet crop, usage was made of the Fast Fourier Transform. Both the frequency and phase of the cosine wave were determined by using ratios between the amplitudes of two adjacent frequency bands of the FFT. By the tests using sine waves and simplified objects it has proven that this is a valid method. However, this is because the amplitudes in the Fourier spectra only contained the contribution of the concerned pattern. If other frequencies occur in the spectrum, as in the spectrum of a beet row will be, this amplitude ratio can be disturbed. From paragraph 3.5.3 about non-discrete frequencies, it can be deduced that when another periodic signal with non-discrete frequency is present in the beet signal, the contribution of it is spread out over a broad range of frequency bands. When some of these contribution ends up in the neighbouring frequency bands that represent the pattern of the beet plants, the ratio of amplitudes is disturbed.

The lookup table that was used to determine the frequency was obtained by using $P(u)$ of neat sine waves. A shortage of this lookup table is that it has difficulty with determining the correct frequency if the frequency of the beets in the signal is discrete. This is because AR has to be zero in this case. Since the signal of a real beet row is less neat than the signal of a sine wave, it would contain multiple (non-

discrete) frequencies apart from the frequency of the beet pattern. Therefore most frequency bands in $P(u)$ are non-zero. A determined AR of zero is therefore exceptional.

Since the total leaf area may not be sprayed with glyphosate, it is of more importance to detect the complete leaf area correctly than detecting the plant stem emerging point. This method determines the beet pattern from full information about the position of the plant leaves perpendicular to the crop row. In fact it estimates the center of the next leaf area, instead of the position of the next plant stem emerging point. This method is therefore better able to determine the position of the leaf area of an individual crop plant as methods that search for the plant stem emerging point or methods that use the geo referential coordinate of the seed that had been recorded during sowing. If for example multiple consecutive beets in a row have grown crooked due to hard winds or a pass of a machine, the leaf area is shifted. With above methods this might result that parts of the leaves are outside the zone which is determined to be beet area, and thus might be sprayed.

In addition to what is stated above, the method to determine the accuracy measures ε and P_{bp} in the image datasets could cause errors. This was because the determined beet position x_{bp} was not always equal to the center of the leaf area, since x_{bp} was determined by appointing the plant stem emerging point in the image (see paragraph 3.3.1). As stated above this was not the desired beet position that was wanted to know. In the simulated datasets x_{bp} was always on the center of the leaf area, so if in the these datasets $\varepsilon = 0$ cm occurs, it was sure that the probability distribution was centered over the concerning beet leaf area.

Detection of plant distance

As a priori information it was added that the seeding distance of the sugar beets will be in the range between 15 and 25 cm. This indicated that the algorithm has to determine the correct frequency from the search area between frequencies of 8 and 14. This limited range was not only needed to send the algorithm in the right direction, but also to prevent that the determined frequency was a plural of the real frequency. This is because in $P(u)$ of a beet row signal, besides the peak of the correct frequency, also peaks can occur at a plural of this frequency. After all these frequencies also correspond to the concerned signal. The frequency range between 8 and 14 was hence a suitable range, since it does not contain any of the plurals of a frequency in the range. This property made it essential to add a limited search area and to ensure that the search area does not contain plurals.

5.3 Results

Accuracy of results

To use the plant pattern as feature to improve the current classification between volunteer potato and sugar beet plants, the regularity of it is of vital importance. Regarding the results it was commonly observed that the next beet position estimation method functioned better for the simulated crop rows from the measurement datasets than for the image datasets. This was for the most part due to the poorer regular plant pattern in the image datasets than in the measurement datasets, as already deduced from the plant distance histograms in Figure 12. From dataset ‘Oudelande’ it was known with certainty that the sugar beets were sown with a precision drill of at least twenty years old. This indicates that a regularity at least comparable to this dataset must be generally feasible.

Figure 30 and Figure 31 respectively show a corresponding and a non-corresponding pattern of the original signal. Both of these iterations provide a next beet position estimate, which both were determined to be correct. Since the beet pattern was not determined correctly in Figure 31, the next beet estimate was based on a non-existing pattern. A drawback of this algorithm is therefore that there is no feedback that approves the presence of the determined beet pattern. With this feedback the relevance of the next beet position estimate could have been determined.

In all simulations like in Figure 32 and Figure 33 it is seen that wrong estimations occur. This could apart from an incorrectly determined plant pattern also be due to an out of pattern next beet. A next beet that is out of pattern cannot be seen in advance. This indicates that it occurred that the pattern was determined correctly, but because the concerned next beet was out of pattern, it was not rated as an accurate estimate. No further investigation was done to quantify the amount of wrong estimates due to an out of pattern next beet or an incorrectly determined plant pattern.

The method to determine if a beet was found or non-found by the algorithm makes that the results for ε look more accurate than they are, because only the found beets were taken into account. With hindsight the determination of found and non-found beets should not have been added, since a large amount of non-found beets would become clear with a higher standard deviation of ε .

After all the number of datasets used was limited. All datasets have about the same plant distance, whereby it is unknown how the algorithm performs on a different plant distance. In practical situations often weeds will appear in the crop row. The datasets contained few weeds, the simulated datasets even no weeds. The robustness of the algorithm to determine the correct pattern was not examined when having weeds in the intensity graph.

Frequency smoothing

Frequency smoothing was used to avoid that the frequency would suddenly change from one iteration to the next. Taking the weighted mean of the current and previous determined frequencies might not be the correct method, since an incorrectly determined frequency continues to be taken into account. Better options would be to take the median or delete the outlying frequencies.

Effect of missing beet plants and an out of pattern object

To determine the effect of missing beet plants and an out of pattern object, just the intensity graph of one iteration was used. This made that the given results were just an indication of the effect of multiple missing plants and out of pattern objects.

With only one beet left in the intensity graph, it is by definition impossible to determine a pattern from a single iteration. But still 43% of the next beet positions were estimated correctly. Most of these estimates however were based on coincidence. The algorithm was set to always determine a pattern with frequency between 8 and 14. Therefore it is likely that close to the next beet position, the next beet was estimated. With only one beet in the intensity graph the algorithm should give no next beet position estimate, or it should extrapolate the last determined pattern of a previous iteration into the current iteration.

The addition of a volunteer potato to the intensity graph was in sense useful, since it is a large disturbance to the beet pattern and therefore it was made more difficult for the algorithm to determine it. The assumption that the volunteer potato overgrows the beet plants is valid, since a potato plant grows faster and higher than a beet plant and widens its leaves.

In the experiments with a missing beet plant and a volunteer potato, no usage was made of frequency smoothing. If this was applied, information would be available from previous iterations in which the pattern might be detected correctly. This might have a positive effect on the number of correctly estimated next beet positions.

6 Conclusions

How regular is the plant pattern in a crop row?

The regularity of the plant pattern differs per dataset. An accuracy of 20.3 ± 2.2 cm is feasible with a common precision sowing machine.

What methods can be used to detect a pattern in a crop row?

The Fast Fourier Transform is found to be a method which is able to detect the pattern of the beet plants in a beet row. This method is able to reveal the frequency and phase of the most present periodicity in the beet row signal. From this frequency and phase a cosine wave could be formed that was overlapped on the original signal of the beet row. The cosine wave can be extrapolated to reveal the estimated next beet positions in the future beet row.

To what extent can the algorithm handle an unknown sowing distance?

When using the Fast Fourier Transformation the algorithm is able to handle an unknown sowing distance, as long as a search area of sowing distances was established. The restriction for the upper (ub) and lower bound (lb) for the search area is that: $ub < 2 * lb$. This is because no plurals of the frequency bands in the Fourier spectrum may be considered.

What is the effect of missing beet plants on the next beet position estimate?

Until three missing beet plants the algorithm was able to estimate 66% of the next beet positions within 3 cm of the real beet position. Since the results were based on experiments on only a single intensity graph, this result is just an indication.

What is the effect of plants that are not in the pattern on the next beet position estimate?

With one volunteer potato plant in the intensity graph the algorithm was able to estimate 71% of the next beet positions within 3 cm of the real beet position. Since in all tests the same intensity graph for the volunteer potato was used and only one intensity graph was used for the whole crop row, this result is just an indication.

Can the regular sowing pattern of a sugar beet crop provide an estimate of the future beet position, in which 68% of the future beet position estimates is within 3 cm of the true beet center point?

For the image datasets on average 70.5% of the actual next beets were found. The position of these found beets was estimated with an average accuracy of 0.0 ± 3.7 cm. Over the six simulated datasets on average 96.2% of the next beets were found. The position of these found beets was estimated with an average accuracy of 0.1 ± 2.4 cm. So when the accuracy measure ϵ is assumed to be normally distributed, by using the simulated datasets it was possible to estimate at least 68% of the future beet positions within 3 cm. For the image datasets this was not possible.

7 Recommendations

Create new image datasets

The new detection and control unit will be mounted on the Husky robot which operates only on one beet row per pass. Therefore first new image datasets should be made containing one crop row. The image datasets should be made on a field having a normal regular beet pattern. Also these images should be made on plots with different sowing distances, weed pressure and growth stage. From these diverse datasets the robustness of the algorithm has to be checked.

Especially when the leaves of consecutive beet plants are overlapping each other, it is hard to distinguish individual beets from a top view image. At this growth stage it might be better to distinguish individual beets when images are made of the side view of the crop row. Possibly a mechanism is needed to lift up the leaves. This enhance the possibility to look under the leaves, having a better visibility on the plant stem emerging point.

Combine with colour features classification

The next beet position estimate has to be added to the current colour-base classification algorithm as a probability of each gridcell (square region of 11 by 11 pix) to contain beet leaves. The current colour-based classification algorithm is able to provide in most cases the correct classification. Therefore the plant position estimate would be especially useful in making a decision if the colour-based classification has not found a clear distinction.

Adapt intensity graph

As seen in Table 12 the presence of a volunteer potato disturbs the intensity graph to such an extent that the beet pattern is often not correctly determined. As the classification algorithm is able to detect a volunteer potato, it is recommended to remove this volunteer potato from the intensity graph, in order to better determine the beet pattern. Also when a missing beet plant is detected, it might be useful to place an object in the intensity graph on this position, such that in subsequent iterations the beet pattern can be determined better.

Probability distribution

The probability distribution has to correspond to the shape of a beet plant. This is because none of the leaves of the beet plant may be sprayed. Therefore a larger distance should have a probability of 1, that corresponds to the size of the beet plants. It has to be investigated if the size of the beet plant can be automatically determined or it has to be added as a priori knowledge.

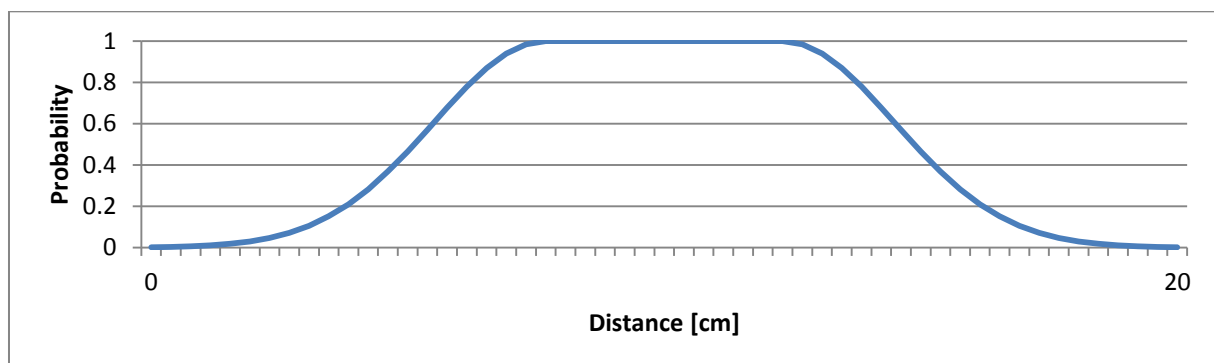


Figure 42: Recommended shape of the probability distribution.

Measure for quality

A quality measure should be added that automatically determines the degree of similarity between the original intensity graph and the corresponding cosine wave. This could be done by determining the percentage of pixels of the original intensity graph which is within the domain where the cosine wave is positive. This percentage must be transformed to act as the degree of similarity, that determines the accuracy of the next beet position estimate. With a low accuracy the probability distribution from Figure 42 must be made wider. This eventually results in that at a certain low accuracy, the total future beet row in the next step is determined to be the possible position of the beet. This method by adapting the width of the probability distribution to the accuracy of the estimate has been described before in paragraph 3.4.3.

Other crops than sugar beets

Besides the usage in a sugar beet crop, this method can be tested in other precision drilled crops. For instance the cultivation of chicory, in which the weed pressure is typically higher than in sugar beets. In this crop it will also be over a longer period possible to determine the plant pattern with this method. It takes longer for the leaves of consecutive chicory plants to overgrow each other, since the crop grows much slower than sugar beets.

References

- Bontsema J., Grift T., Pleijsier K. (1991) *Mechanical weed control in sugar beet growing: The detection of a plant in a row*. IFAC/ISHS workshop. Matsuyama, Japan. Sept 30 - Oct 3, 1991.
- Bontsema J., Van Asselt C.J., Lempens P.W.J., Van Straten G. (1998) *Intra-row weed control: a mechatronics approach*. 1st IFAC Workshop on control applications and ergonomics in agriculture. Athens, Greece. June 15-17, 1998.
- Campen O. van. (2009) *Aardappelopslag in suikerbieten*. Retrieved on 17-06-2013 from: <http://www.kennisakker.nl/actueel/kennistekst/aardappelopslag-suikerbieten>
- CBS. (2012) *Productie van akkerbouwgewassen naar regio*, Centraal Bureau voor de Statistiek, Den Haag/Heerlen.
- ClearpathRobotics. (2013) *Husky Technical Specifications*. Retrieved on 19-06-2013 from: <http://www.clearpathrobotics.com/husky/tech-specs/>
- Gonzalez R.C., Woods R.E. (2008) *Digital Image Processing*. Third ed. Pearson Education, Upper Saddle River, New Jersey.
- Hemming J., Nieuwenhuizen A.T., Struik L.E. (2011) *Image analysis system to determine crop row and plant positions for an intra-row weeding machine*. CIGR International Symposium on Sustainable Bioproduction. Tokyo, Japan. Sept 19-23, 2011.
- IRS. (2000) *Invloed van rastype en plantaantal op interne en externe kwaliteit van suikerbieten*, Jaarverslag 2000, IRS.
- IRS. (2011) *Zaaiafstand en standdichtheid*, Teelthandleiding, IRS.
- Jager M.G. de. (2013) *Colour constancy in machine vision under varying natural lighting conditions*. MSc Thesis at Farm Technology Group. Wageningen University.
- Midtiby H. S., Giselsson T. M., Jørgensen R. N. (2012) *Estimating the plant stem emerging points (PSEPs) of sugar beets at early growth stages*. *Biosystems Engineering* 111: 83-90.
- Midtiby H.S. (2012) *Real time computer vision technique for robust plant seedling tracking in field environment*. PhD Thesis at Faculty of Engineering, Institute of Chemical Engineering, Biotechnology and Environmental Technology. University of Southern Denmark.
- Nieuwenhuizen A.T. (2009) *Automated detection and control of volunteer potato plants*. PhD Thesis at Farm Technology Group. Wageningen University.
- Nieuwenhuizen AT, Hofstee JW, van Henten EJ. (2009) *Real-time unsupervised adaptive Bayesian classification for weed plant detection in arable fields*. *Automated detection and control of volunteer potato plants*: 71-94.
- Nørremark M., Griepentrog H. W., Nielsen J., Søgaard H. T. (2008) *The development and assessment of the accuracy of an autonomous GPS-based system for intra-row mechanical weed control in row crops*. *Biosystems Engineering* 101: 396-410.
- Shrestha D. S., Steward B. L., Birrell S. J. (2004) *Video Processing for Early Stage Maize Plant Detection*. *Biosystems Engineering* 89: 119-129.
- Steward Brian L., Tian Lei F. (1999) *Real-time weed detection in outdoor field conditions*. *Proceedings of SPIE - The International Society for Optical Engineering* 3543: 266-278.
- Tang L., Tian L. F. (2008) *Plant identification in mosaicked crop row images for automatic emerged corn plant spacing measurement*. *Transactions of the ASABE* 51: 2181-2191.
- Veerman A. (2003) *Teelthandleiding consumptieaardappelen - ziekten en plagen*. Retrieved on 12-06-2013 from: <http://www.kennisakker.nl/node/167#Opslag>
- Vollebregt M. (2013) *Texture based discrimination between sugar beet and volunteer potato*. MSc Thesis at Farm Technology Group. Wageningen University.
- Woebbecke D. M., Meyer G. E., Von Bargen K., Mortensen D. A. (1995) *Color indices for weed identification under various soil, residue, and lighting conditions*. *Transactions of the American Society of Agricultural Engineers* 38: 259-269.

Appendix

Appendix A	iii
Appendix B	v
Appendix C	vi
Appendix D	x
Appendix E.....	xiii
Appendix F.....	xvi
Appendix G	xvii
Appendix H	xix
Appendix I.....	xx

Appendix A

Table 13: Measurement data of dataset ‘Munnekezijl’ containing positions of beet plants measured from the first beet plant in the row.

Test field: Munnekezijl		date: 07-06-2006		
Plant number	row 1 (cm)	row 2 (cm)	row 3 (cm)	row 4 (cm)
1	0	0	0	0
2	12	15	17	18
3	32	32	33	36
4	48	51	53	55
5	67	69	71	72
6	85	89	91	91
7	102	104	108	108
8	121	124	128	129
9	140	142	144	145
10	158	160	180	164
11	175	181	198	182
12	194	200	218	201
13	211	216	254	219
14	228	234	288	237
15	247	252	308	258
16	265	271	326	291
17	282	289	362	310
18	303	308	382	328
19	320	326	418	348
20	337	343	438	365
21	356	362	454	402
22	374	380	471	420
23	392	400	490	439
24	413	418	509	455
25	429	437	526	474
26	446	452	544	494
27	464	472	564	512
28	485	491	598	528
29	520	509	616	548
30	539	528	635	567
31	555	547	651	584
32	574	565	671	599
33	610	582	689	619
34	627	601	711	638
35	646	620	725	678
36	665	638	744	692
37	683	654	761	730
38	699	671	781	748
39	719	692	798	768
40	737	709	818	784
41	753	727	835	802
42	773	748	851	822
43	791	763	873	839
44	809	784	888	858
45	826	801	907	875
46	846	820	925	891
47	864	839	943	911
48	882	875	962	930
49	900	894	999	965
50	917	914		984
51	935	931		
52	953	950		
53	973	966		
54	990	988		

Appendix

Table 14: Measurement data of dataset ‘Oudelande’ containing positions of beet plants measured from a base position.

Location: Oudelande			
Date: 29-04-2013			
Plant number	row 1 [cm]	row 2 [cm]	row 3 [cm]
1	4	0	28
2	22	17	91
3	44	38	109
4	86	57	129
5	108	80	151
6	126	99	192
7	166	119	212
8	187	142	231
9	209	162	253
10	250	183	272
11	269	221	293
12	290	242	315
13	310	263	334
14	329	285	354
15	354	303	373
16	375	325	415
17	393	346	436
18	412	365	457
19	435	383	476
20	455	407	497
21	474	428	517
22	496	448	541
23	515	466	557
24	537	489	578
25	557	511	596
26	573	529	616
27	595	551	658
28	615	571	697
29	637	591	719
30	675	609	736
31	695	631	759
32	736	650	796
33	756	672	817
34	797	686	840
35	819	711	857
36	858	730	879
37	879	750	899
38	900	767	922
39	940	790	937
40	958	809	963
41	980	830	986
42	1000	850	1003
43	1019	870	1023
44	1042	892	1042
45		911	
46		930	
47		954	
48		970	
49		996	
50		1010	
51		1036	

Appendix B

Table 15: A random series of data points, representing the position of nine beet plants.

Beet place number	Beet plant position [cm]
0	0
1	18
2	44
3	60
4	83
5	104
6	117
7	147
8	161

Appendix C

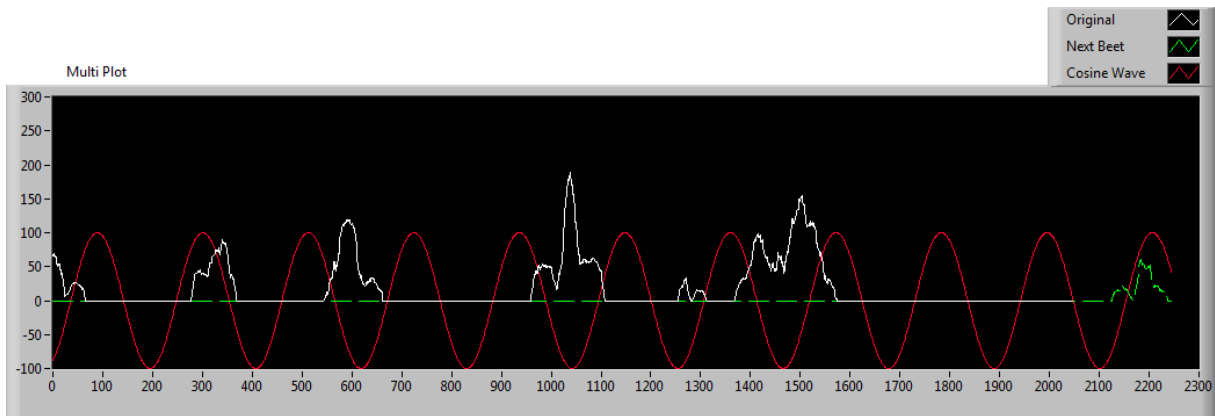


Figure 43: Random original signal from dataset 2008-05-28 Clay Soil (white line), corresponding cosine wave with properties $f_e = 9.67$ and $\varphi_e = 208^\circ$ (red line) and next iteration intensity graph (green line).

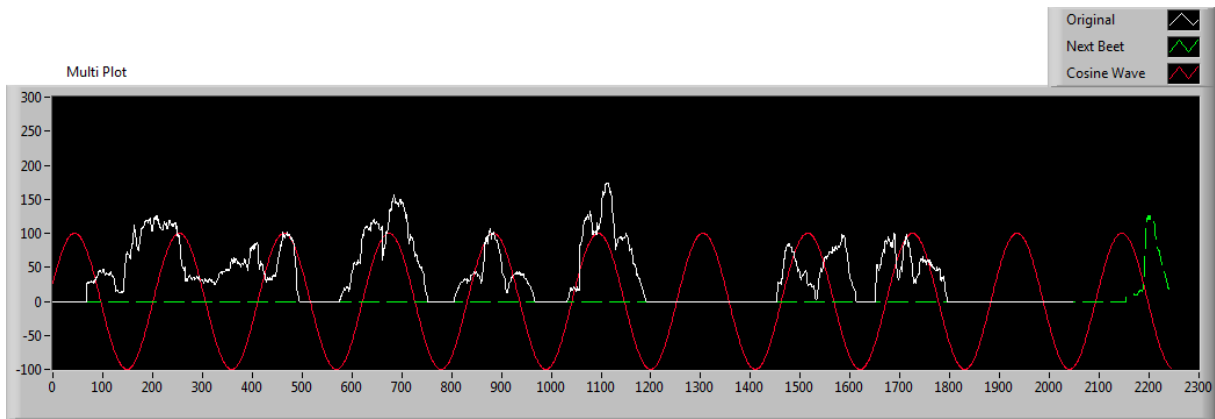


Figure 44: Random original signal from dataset 2008-05-28 Clay Soil (white line), corresponding cosine wave with properties $f_e = 9.74$ and $\varphi_e = 285^\circ$ (red line) and next iteration intensity graph (green line).

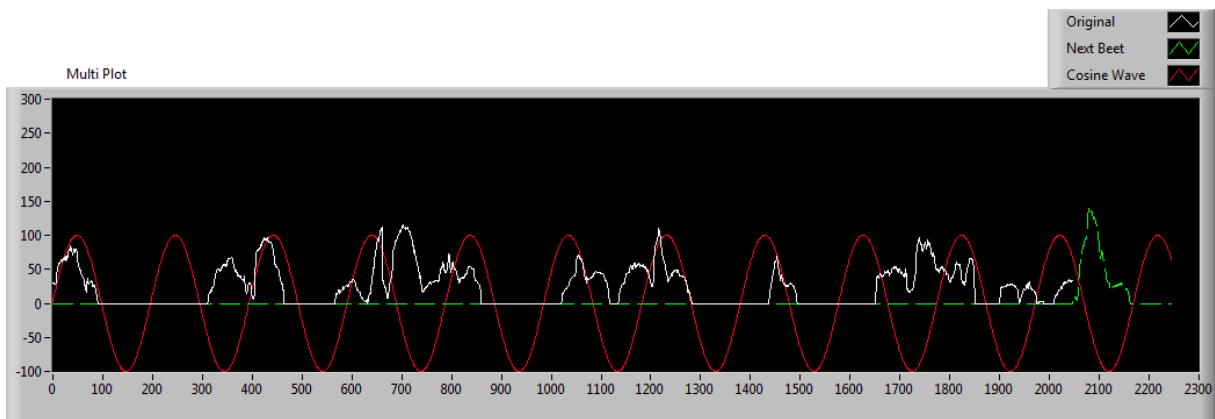


Figure 45: Random original signal from dataset 2008-05-28 Clay Soil (white line), corresponding cosine wave with properties $f_e = 10.38$ and $\varphi_e = 272^\circ$ (red line) and next iteration intensity graph (green line).

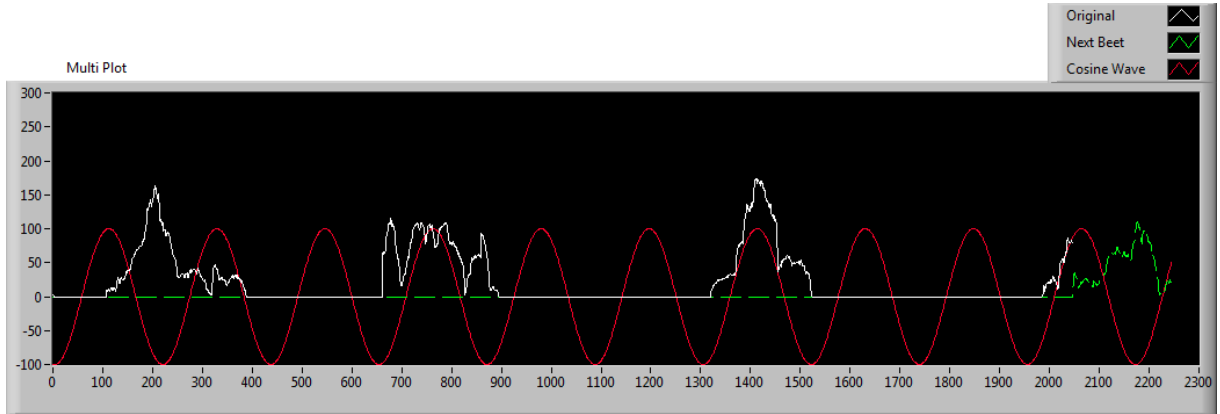


Figure 46: Random original signal from dataset 2008-05-28 Clay Soil (white line), corresponding cosine wave with properties $f_e = 9.44$ and $\varphi_e = 174^\circ$ (red line) and next iteration intensity graph (green line).

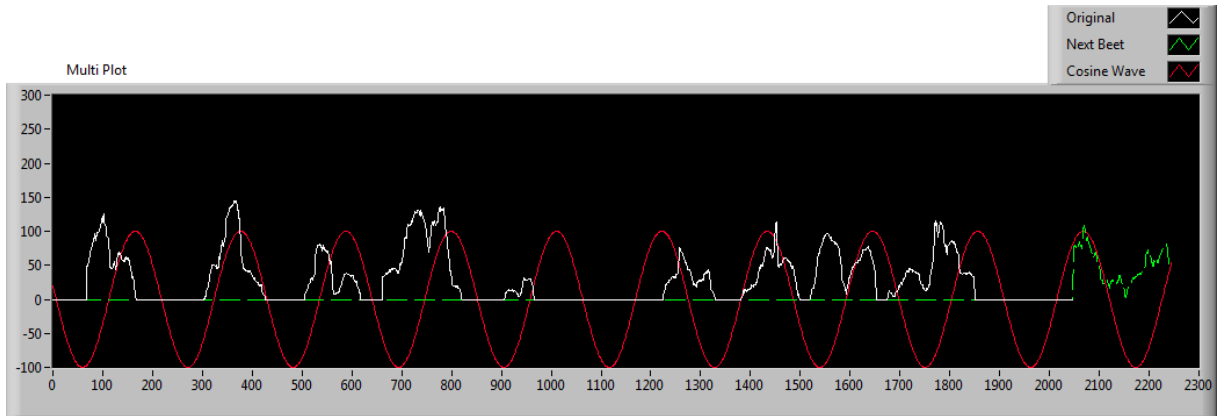


Figure 47: Random original signal from dataset 2008-05-28 Clay Soil (white line), corresponding cosine wave with properties $f_e = 9.69$ and $\varphi_e = 79^\circ$ (red line) and next iteration intensity graph (green line).

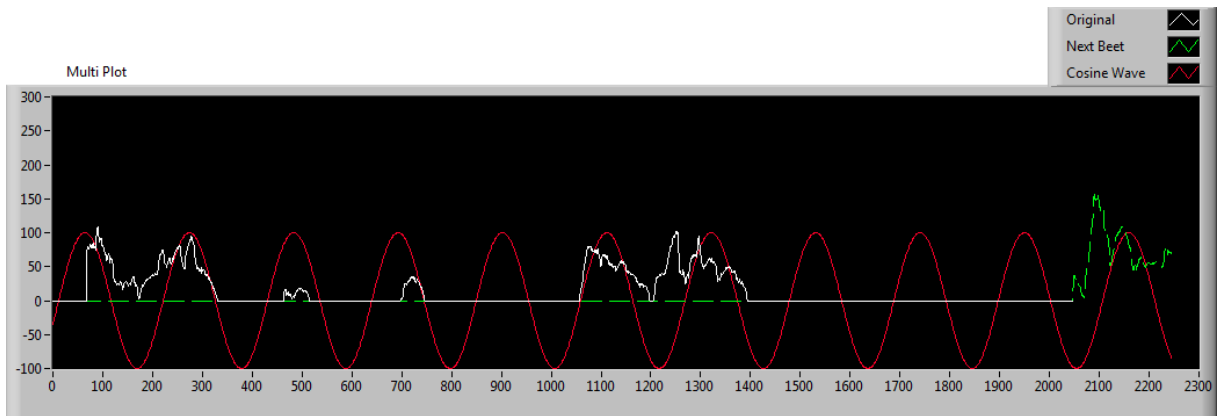


Figure 48: Random original signal from dataset 2008-05-28 Sand Soil (white line), corresponding cosine wave with properties $f_e = 9.78$ and $\varphi_e = 250^\circ$ (red line) and next iteration intensity graph (green line).

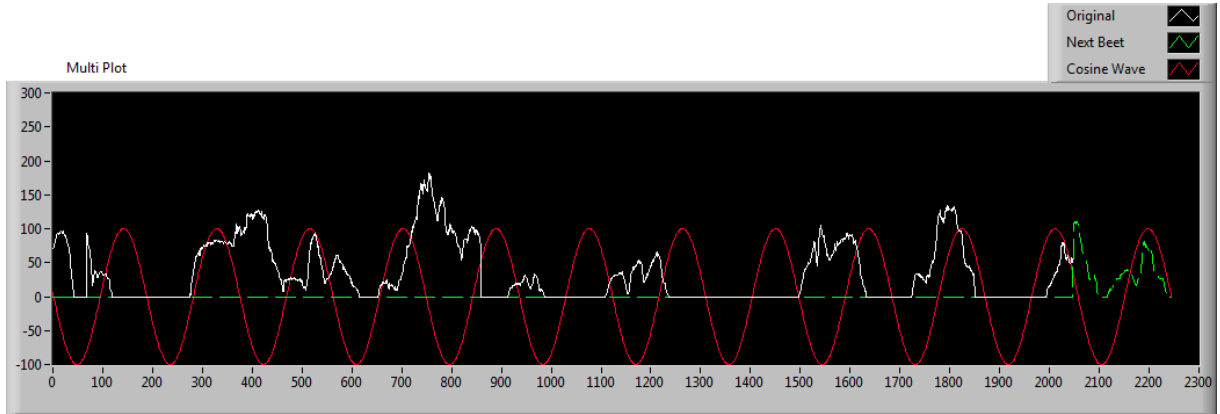


Figure 49: Random original signal from dataset 2088-05-28 Sand Soil (white line), corresponding cosine wave with properties $f_e = 10.96$ and $\varphi_e = 87^\circ$ (red line) and next iteration intensity graph (green line).

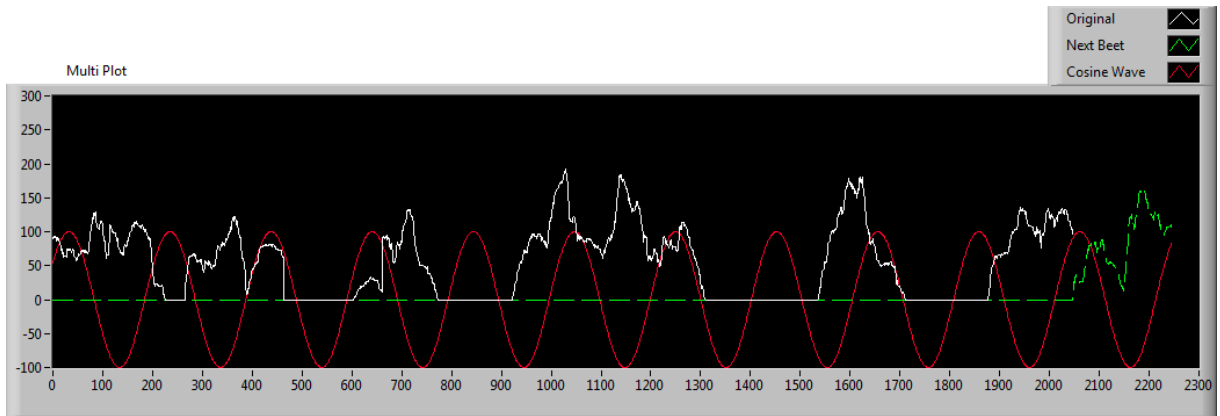


Figure 50: Random original signal from dataset 2088-05-28 Sand Soil (white line), corresponding cosine wave with properties $f_e = 10.09$ and $\varphi_e = 303^\circ$ (red line) and next iteration intensity graph (green line).

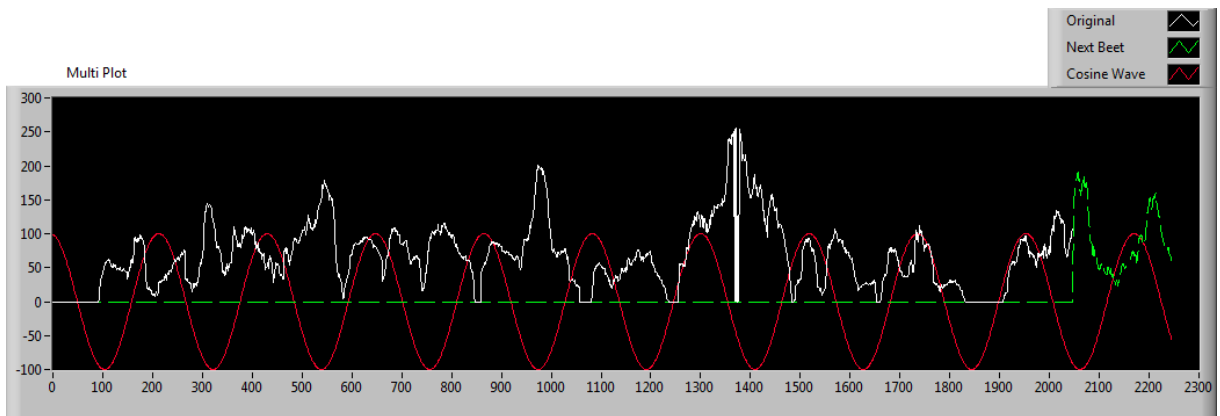


Figure 51: Random original signal from dataset 2088-05-28 Sand Soil (white line), corresponding cosine wave with properties $f_e = 9.42$ and $\varphi_e = 8^\circ$ (red line) and next iteration intensity graph (green line).

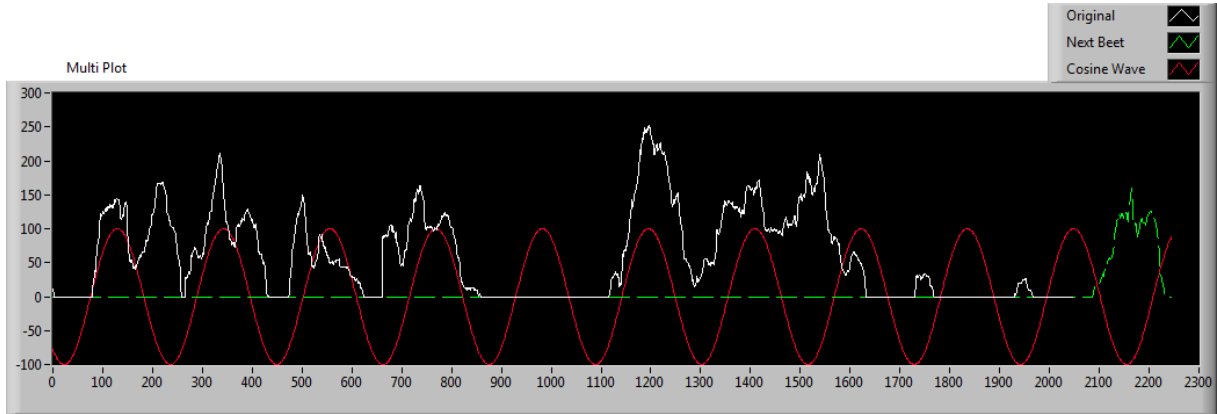


Figure 52: Random original signal from dataset 2008-06-02 Clay Soil (white line), corresponding cosine wave with properties $f_e = 9.60$ and $\varphi_e = 142^\circ$ (red line) and next iteration intensity graph (green line).

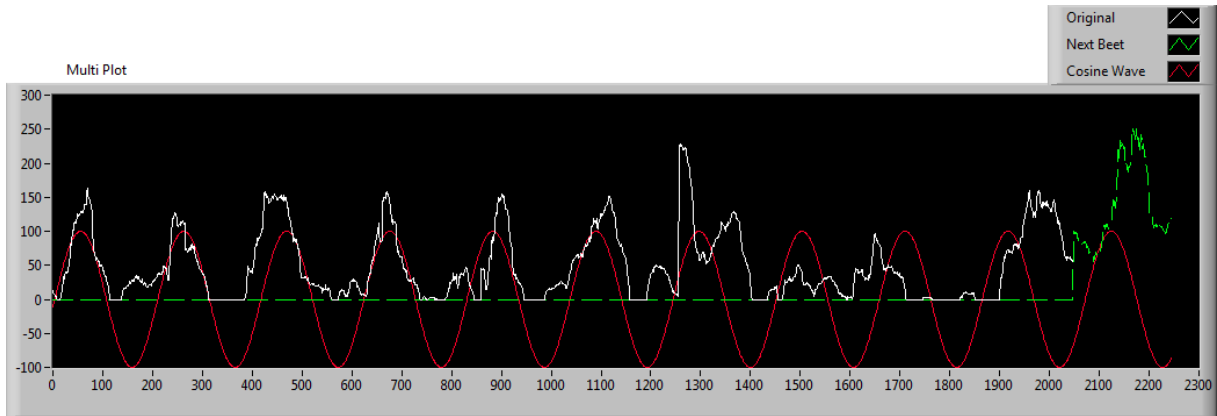


Figure 53: Random original signal from dataset 2008-06-02 Clay Soil (white line), corresponding cosine wave with properties $f_e = 9.90$ and $\varphi_e = 263^\circ$ (red line) and next iteration intensity graph (green line).

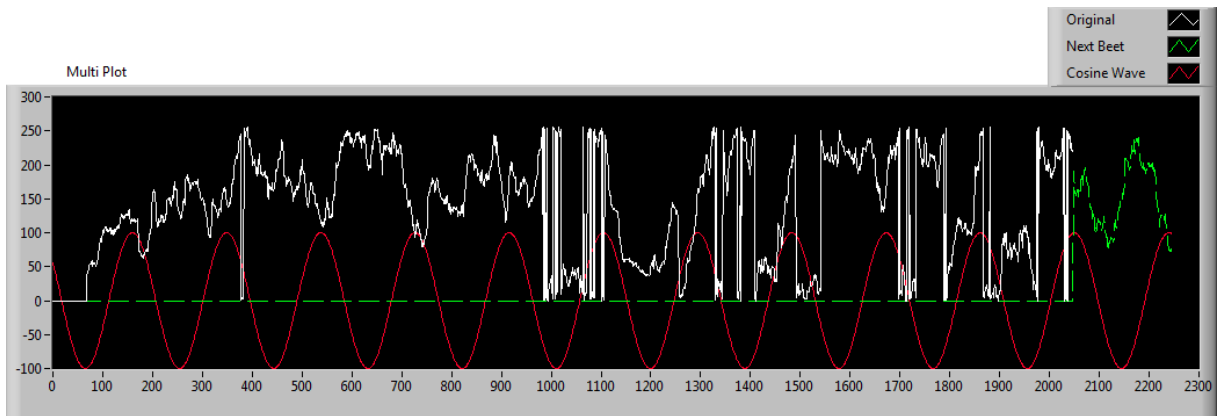


Figure 54: Random original signal from dataset 2008-06-02 Sand Soil (white line), corresponding cosine wave with properties $f_e = 10.83$ and $\varphi_e = 56^\circ$ (red line) and next iteration intensity graph (green line). This iteration contained a lot of overlapping beets.

Appendix D

Table 16: Independent samples T-Test on ε between case with and without frequency smoothing for simulation 1 of dataset 'Oudelande'.

		Levene's Test for Equality of Variances		t-test for Equality of Means						
		F	Sig.	t	df	Sig. (2-tailed)	Mean Difference	Std. Error Difference	95% Confidence Interval of the Difference	
									Lower	Upper
Difference	Equal variances assumed	.431	.512	-.319	247	.750	-.11059	.34676	-.79357	.57238
	Equal variances not assumed			-.319	246.546	.750	-.11059	.34668	-.79343	.57225

Table 17: Independent samples T-Test on ε between case with and without frequency smoothing for simulation 2 of dataset 'Oudelande'.

		Levene's Test for Equality of Variances		t-test for Equality of Means						
		F	Sig.	t	df	Sig. (2-tailed)	Mean Difference	Std. Error Difference	95% Confidence Interval of the Difference	
									Lower	Upper
Difference	Equal variances assumed	3.011	.084	-.100	250	.920	-.03300	.32980	-.68253	.61653
	Equal variances not assumed			-.100	246.215	.920	-.03300	.32980	-.68258	.61658

Table 18: Independent samples T-Test on ε between case with and without frequency smoothing for simulation 3 of dataset ‘Oudelande’.

		Levene's Test for Equality of Variances		t-test for Equality of Means						
		F	Sig.	t	df	Sig. (2-tailed)	Mean Difference	Std. Error Difference	95% Confidence Interval of the Difference	
									Lower	Upper
Difference	Equal variances assumed	4.243	.040	.141	250	.888	.04835	.34320	-.62759	.72429
	Equal variances not assumed			.141	246.899	.888	.04835	.34242	-.62608	.72279

Table 19: Independent samples T-Test on ε between case with and without frequency smoothing for simulation 1 of dataset ‘Munnekezijl’.

		Levene's Test for Equality of Variances		t-test for Equality of Means						
		F	Sig.	t	df	Sig. (2-tailed)	Mean Difference	Std. Error Difference	95% Confidence Interval of the Difference	
									Lower	Upper
Difference	Equal variances assumed	.457	.499	.238	367	.812	.05805	.24410	-.42196	.53805
	Equal variances not assumed			.238	366.011	.812	.05805	.24418	-.42212	.53821

Table 20: Independent samples T-Test on ε between case with and without frequency smoothing for simulation 2 of dataset ‘Munnekezijl’.

		Levene's Test for Equality of Variances		t-test for Equality of Means						
		F	Sig.	t	df	Sig. (2-tailed)	Mean Difference	Std. Error Difference	95% Confidence Interval of the Difference	
									Lower	Upper
Difference	Equal variances assumed	3.122	.078	.762	368	.447	.18034	.23681	-.28533	.64601
	Equal variances not assumed			.762	366.503	.447	.18034	.23671	-.28515	.64583

Table 21: Independent samples T-Test on ε between case with and without frequency smoothing for simulation 3 of dataset ‘Munnekezijl’.

		Levene's Test for Equality of Variances		t-test for Equality of Means						
		F	Sig.	t	df	Sig. (2-tailed)	Mean Difference	Std. Error Difference	95% Confidence Interval of the Difference	
									Lower	Upper
Difference	Equal variances assumed	1.238	.267	.064	369	.949	.01408	.21837	-.41533	.44349
	Equal variances not assumed			.064	368.739	.949	.01408	.21835	-.41530	.44345

Appendix E

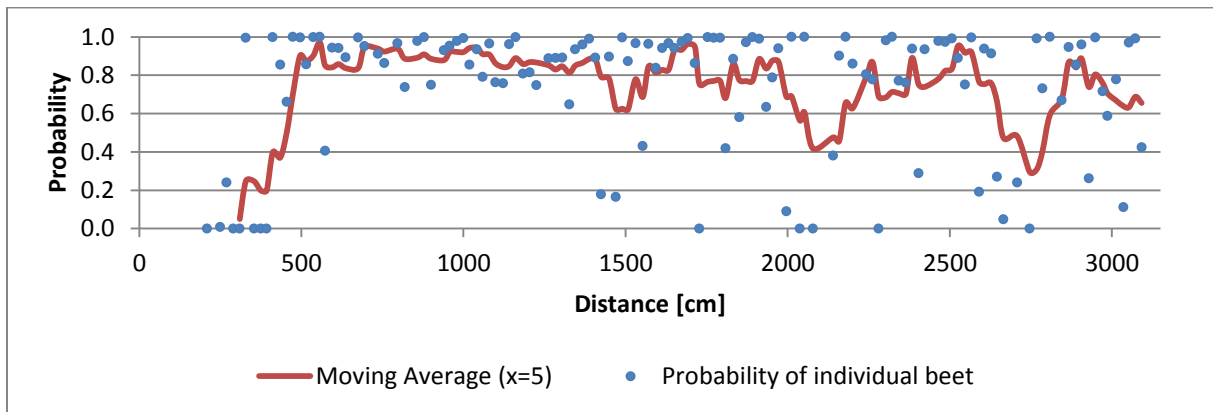


Figure 55: Determined probabilities P by the next beet estimation at the beet positions x_{bp} from dataset ‘Oudelande’ for simulation 2 (blue points). Red line represents the moving average of P with $x = 5$.

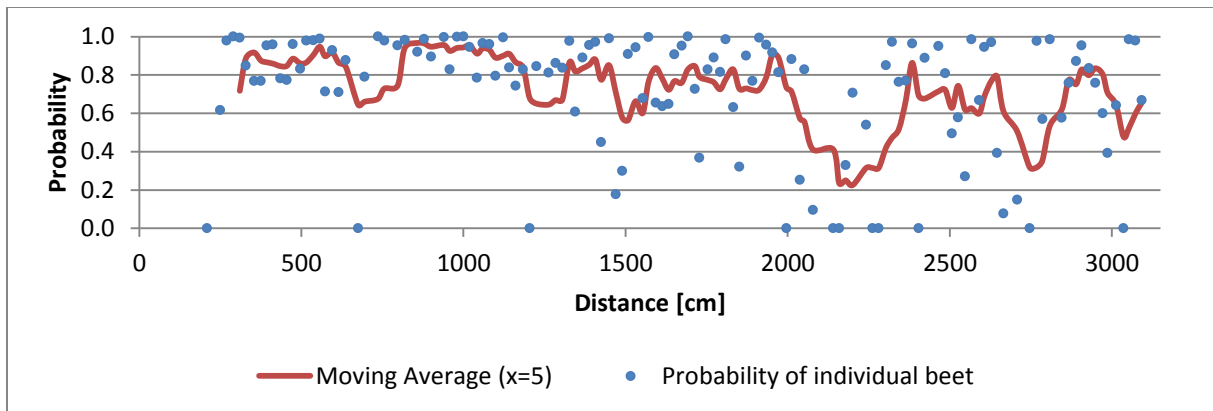


Figure 56: Determined probabilities P by the next beet estimation at the beet positions x_{bp} from dataset ‘Oudelande’ for simulation 3 (blue points). Red line represents the moving average of P with $x = 5$.

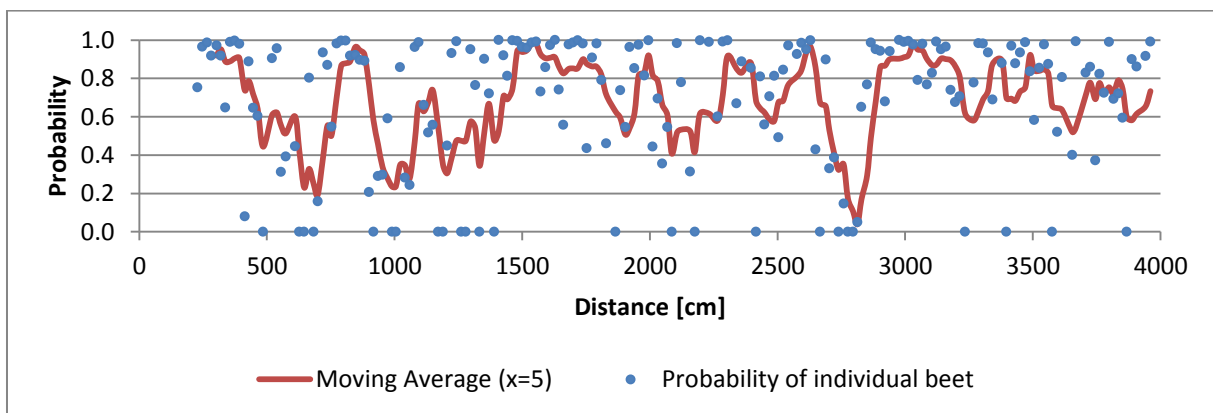


Figure 57: Determined probabilities P by the next beet estimation at the beet positions x_{bp} from dataset ‘Munnekezijl’ for simulation 2 (blue points). Red line represents the moving average of P with $x = 5$.

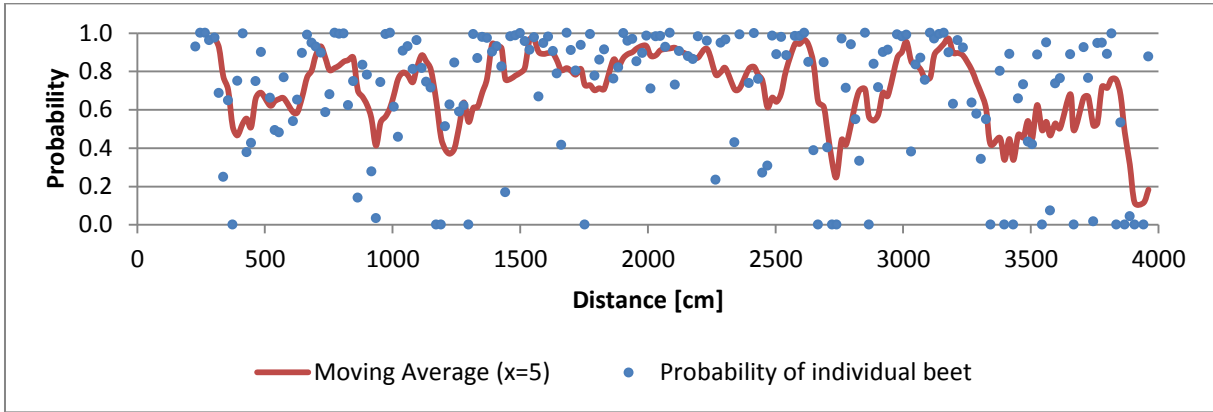


Figure 58: Determined probabilities P by the next beet estimation at the beet positions x_{pp} from dataset 'Munnekezijl' for simulation 3 (blue points). Red line represents the moving average of P with $x = 5$.

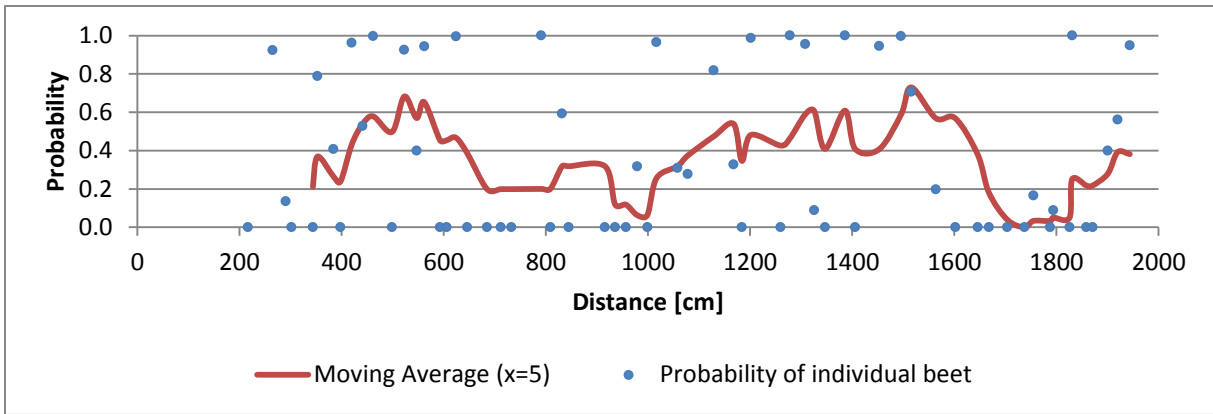


Figure 59: Determined probabilities P by the next beet estimation at the beet positions x_{pp} from dataset '2008-05-28 Clay Soil' for the middle row (blue points). Red line represents the moving average of P with $x = 5$.

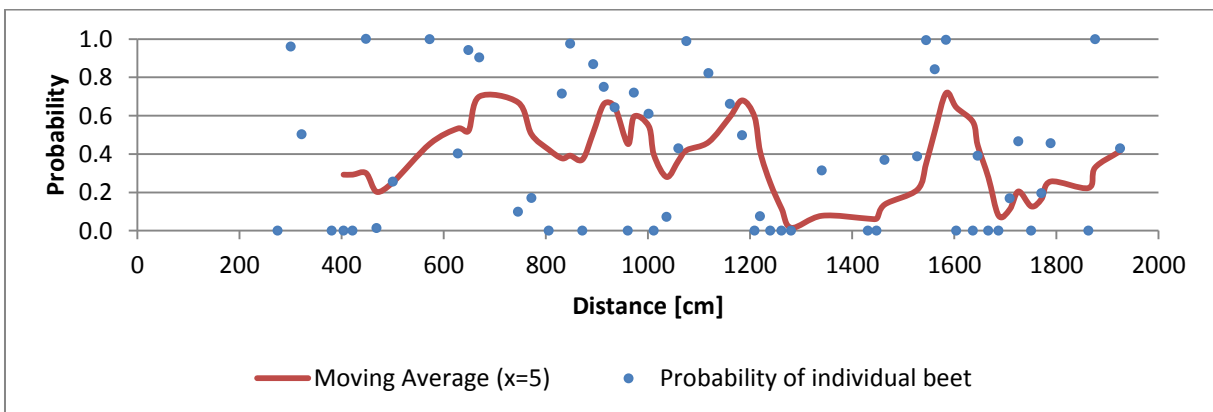


Figure 60: Determined probabilities P by the next beet estimation at the beet positions x_{pp} from dataset '2008-05-28 Clay Soil' for the right row (blue points). Red line represents the moving average of P with $x = 5$.

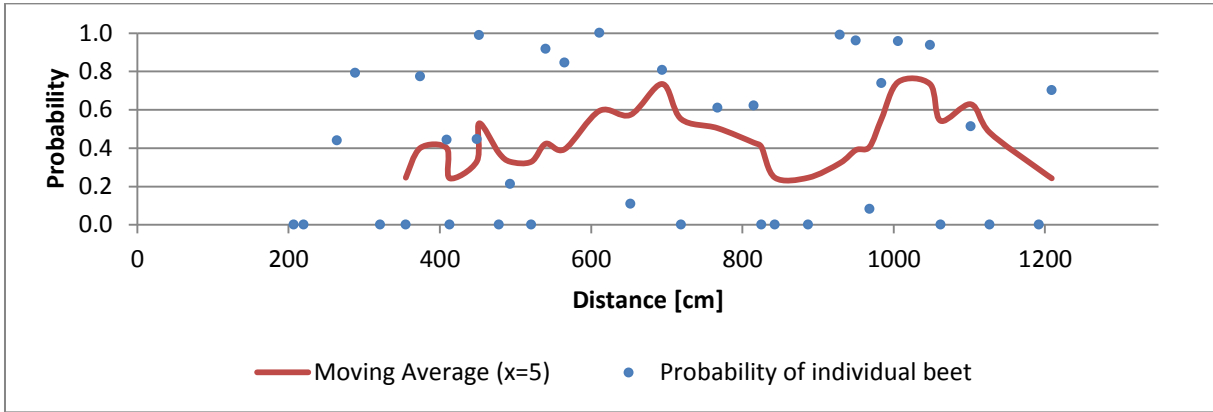


Figure 61: Determined probabilities P by the next beet estimation at the beet positions x_{pp} from dataset '2008-06-02 Clay Soil' for the middle row (blue points). Red line represents the moving average of P with $x = 5$.

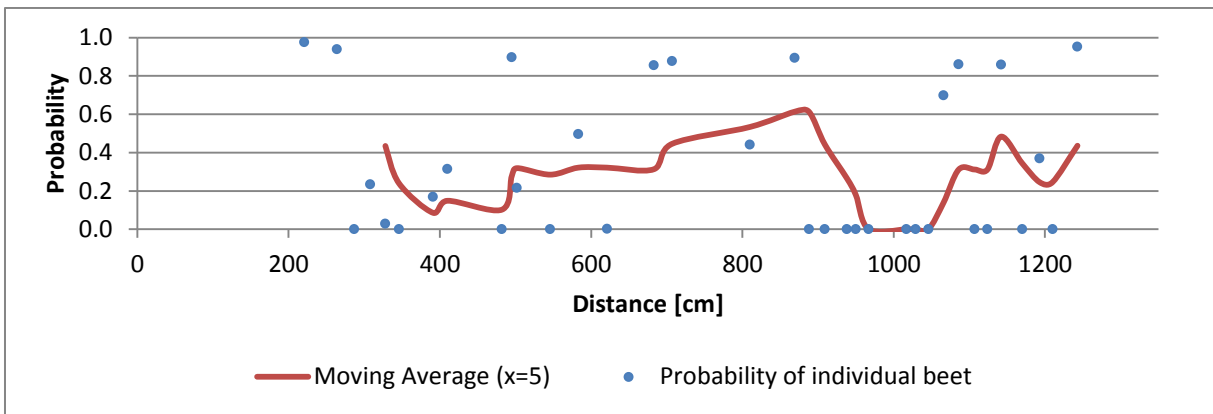


Figure 62: Determined probabilities P by the next beet estimation at the beet positions x_{pp} from dataset '2008-06-02 Clay Soil' for the right row (blue points). Red line represents the moving average of P with $x = 5$.

Appendix F

Table 22: Counts in the ranges of ε and P_{bp} for the intensity graphs with volunteer potato.

ε	Count	P_{bp}	Count
[-6.0;-5.5>	0	<0.0;0.1]	2
[-5.5;-5.0>	0	<0.1;0.2]	4
[-5.0;-4.5>	0	<0.2;0.3]	6
[-4.5;-4.0>	0	<0.3;0.4]	0
[-4.0;-3.5>	0	<0.4;0.5]	0
[-3.5;-3.0>	0	<0.5;0.6]	6
[-3.0;-2.5>	0	<0.6;0.7]	19
[-2.5;-2.0>	13	<0.7;0.8]	40
[-2.0;-1.5>	27	<0.8;0.9]	65
[-1.5;-1.0>	32	<0.9;1.0]	235
[-1.0;-0.5>	63		
[-0.5;0.0>	99		
<0.0;0.5]	59		
<0.5;1.0]	17		
<1.0;1.5]	11		
<1.5;2.0]	8		
<2.0;2.5]	7		
<2.5;3.0]	21		
<3.0;3.5]	1		
<3.5;4.0]	7		
<4.0;4.5]	0		
<4.5;5.0]	5		
<5.0;5.5]	5		
<5.5;6.0]	0		

Appendix G

The Fast Fourier Transformation (FFT) is a fast method to calculate the Discrete Fourier Transformation (DFT). The number of calculations is reduced from N^2 to $N \log_2 N$. Especially at large N , this results in a major decrease of computational load. However, using FFT restricts that the input vector has to have a size of a power of 2 (Gonzalez and Woods, 2008). The algorithm was developed by James Cooley and John Tukey in 1965. The bottom line is that the transformation is split such that two recursive calculations appear, that both make a smart use of the periodicity and symmetry in the sine/cosine functions. Eventually the FFT results in the same outcome as the DFT.

In below section some key characteristics of the DFT were listed that were important for this research. These characteristics were derived from the book ‘ Digital image processing ’ by Gonzalez & Woods (2008).

The one dimensional Fourier transform is determined by the function:

$$F(u) = \sum_{x=0}^{M-1} f(x) e^{-j2\pi(\frac{ux}{M})} \quad [-] \quad (22)$$

In which $f(x)$ is the original function and M is the length of the signal. The Fourier spectrum of a signal has the same size as the original signal. So the length of the spatial value x is equal to the length of the frequency-domain variable u . A large amplitude in the spectrum implies a greater prominence of a sinusoid of that certain frequency. The inverse of equation (10) is defined as:

$$\bar{f}(x) = \frac{1}{M} \sum_{u=0}^{M-1} F(u) e^{j2\pi(\frac{ux}{M})} \quad [\text{pix}] \quad (23)$$

The Fourier (or frequency) spectrum is given by a real and imaginary part, since the Fourier Transform is a complex value:

$$|F(u)| = [R^2(u) + I^2(u)]^{\frac{1}{2}} \quad [-] \quad (24)$$

In which R and I stand for the real and imaginary parts of the Fourier transform, respectively. The phase angle contains shape information of the signal. It is described as:

$$\varphi(u) = \arctan \left[\frac{I(u)}{R(u)} \right] \quad [^\circ] \quad (25)$$

The four-quadrant arctangent has to be used to calculate the phase angle. Finally, the power spectrum is defined as:

$$P(u) = R^2(u) + I^2(u) \quad [-] \quad (26)$$

$P(u)$ can be used to eliminate the imaginary part. The Fourier transform exhibits conjugate symmetry. The spectrum is even symmetric about the origin:

$$|F(u)| = |F(-u)| \quad [-] \quad (27)$$

Contrary, the phase angle exhibits odd symmetry about the origin:

$$\varphi(u) = -\varphi(-u) \quad [^\circ] \quad (28)$$

Regarding equation (10) the zero frequency term is proportional to the average value of the signal $f(x)$, since $F(0) = \sum_{x=0}^{M-1} f(x)$. This results in the sum of all function values. The average $\bar{f}(x)$ is obtained by dividing $F(0)$ with M . In formula: $F(0) = M\bar{f}(x)$. It is also called the dc term.

The Fourier transform and also the inverse are both periodic according to below equations:

$$F(u) = F(u + kM) \quad [-] \quad (29)$$

$$\bar{f}(x) = \bar{f}(x + kM) \quad [\text{pix}] \quad (30)$$

In which k is an integer ($k = 0, 1, \dots, n$).

Appendix H

Below an example was elaborated that clarifies the steps to determine the frequency from a given power spectrum as seen in Figure 63.

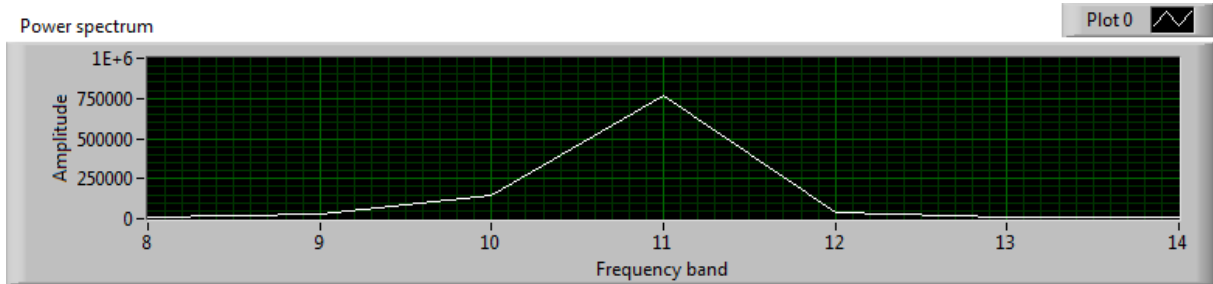


Figure 63: Random power spectrum of a signal, used to determine frequency of the original signal with the method described in this paragraph.

1. $u_{max} = 11$, since it is the highest amplitude in $P(u)$.
2. $Side = \text{Max}\{P(10), P(12)\}$; $Side = \text{Max}\{145339, 39678\}$; So $Side = P(10)$.
3. $AR = \frac{145339}{765514} = 0.190$.
4. $Side = P(10) = u_{max} - 1$, so from the lookup table the interval $[10.5; 11]$ has to be selected.
5. From the lookup table it followed that $f_e = 10.700$. This is depicted in Figure 64.

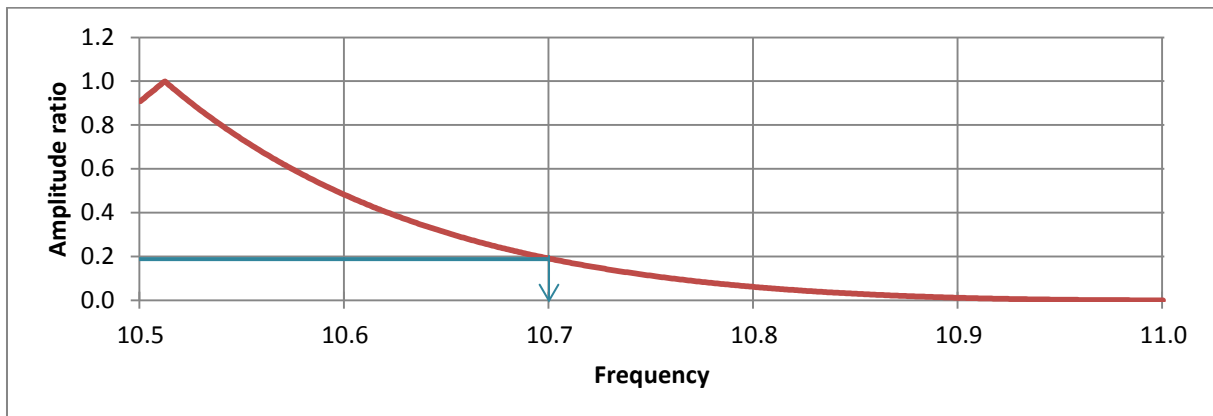


Figure 64: Interval between 10.5 and 11.0 of the amplitude ratio plotted against the sine wave frequency (red line). The blue line indicates that at an AR of 0.190 corresponds to a frequency of 10.7

Appendix I

Below it was clarified how the phase angle was determined from an intensity graph. In Figure 65 a random intensity graph is seen, with $d = 196$ pix and $ts = hs = 0$ pix. The graph was transformed using FFT to $F(u)$ (Figure 66). The frequency of the original signal was estimated to be 10.47 (determined using the steps to determine the frequency).

$$f_e = 10.47 \rightarrow n = 10 \text{ and } (n + 1) = 11$$

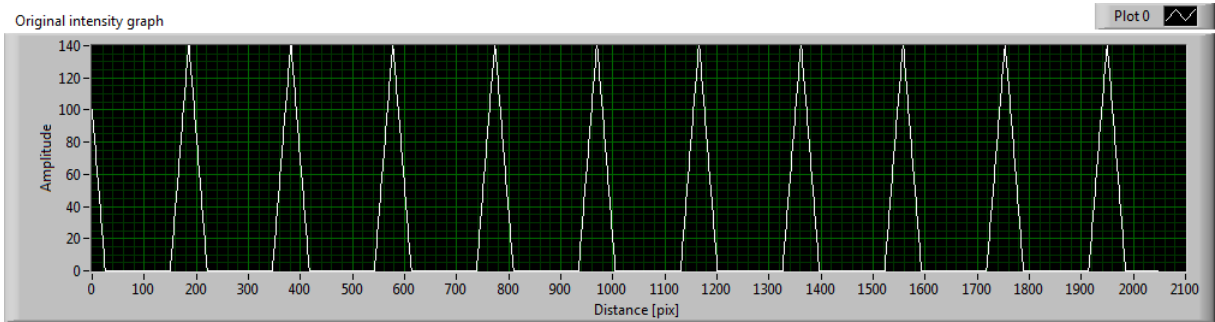


Figure 65: A random simplified crop row with $d = 196$ pix and $ts = hs = 0$ pix having an unknown phase. The estimated frequency is 10.47.

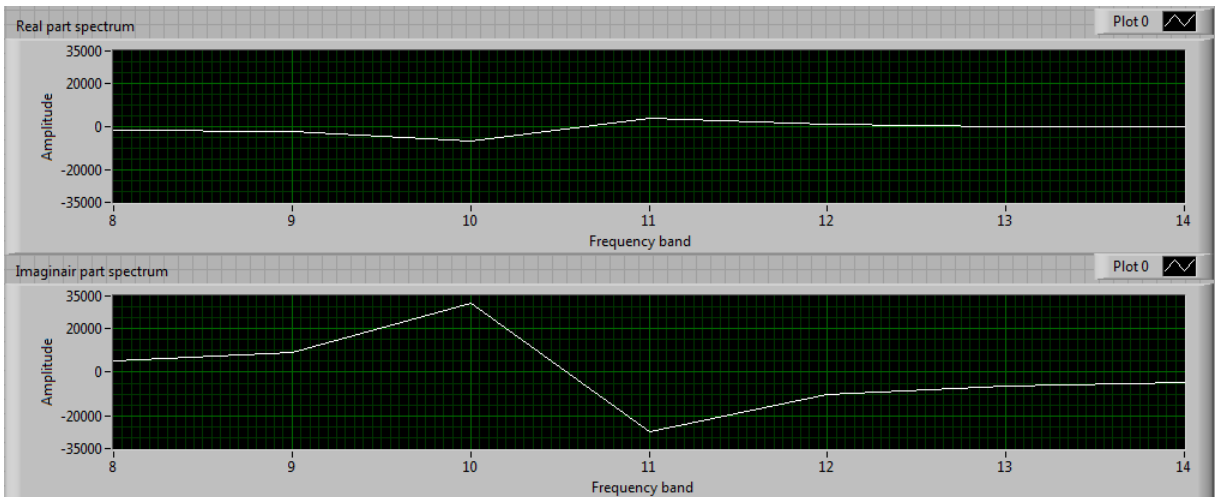


Figure 66: $R(u)$ (above graph) and $I(u)$ (below graph) of the intensity graph from Figure 65.

First $\varphi(n)$ and $\varphi(n + 1)$ were determined.

$$\varphi(10) = \arctan \left[\frac{31841}{-6500} \right] = 101.54^\circ$$

$$\varphi(11) = \arctan \left[\frac{-27175}{3996} \right] = -81.64^\circ$$

$$r_{o\varphi(10)} = 1 - (10.47 - 10) = 0.53$$

$$r_{o\varphi(11)} = 10.47 - 10 = 0.47$$

$$\varphi_e = 0.53 * 101.54 + 0.47 * -81.64 = 15.45^\circ$$

A sine with frequency $f_e = 10.47$, phase angle $\varphi_e = 15.45$ and amplitude of 100 was overlaid over the original intensity graph (Figure 67).

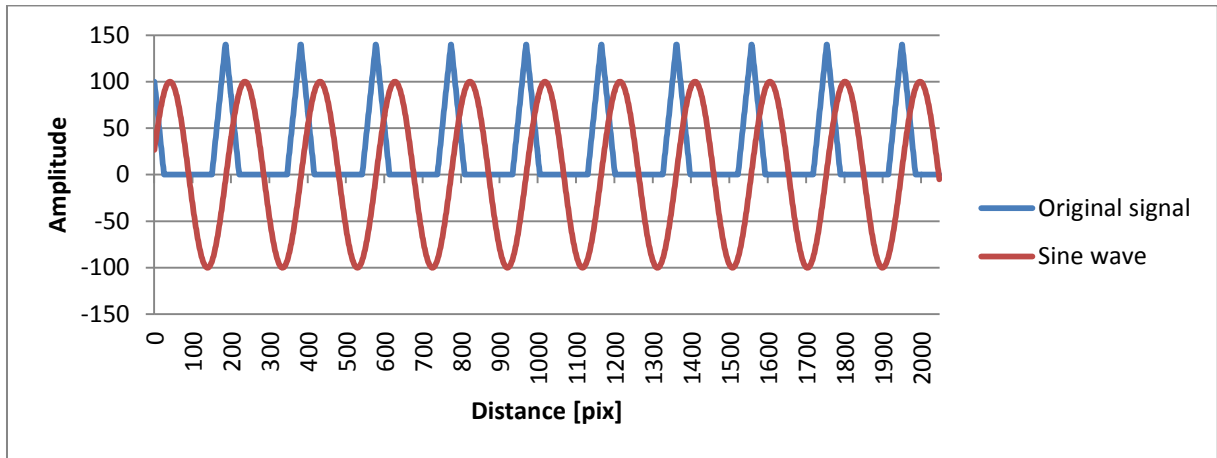


Figure 67: Original intensity graph from Figure 65 (blue line) overlaid with a sine wave having frequency $f_e = 10.47$, phase angle $\varphi_e = 15.45$ and amplitude of 100 (red line).

From Figure 67 it can be seen that the peaks of the sine wave does not correspond to the peaks of the original signal. It was found that φ_e must be increased by 90° to match the peaks of the wave and the original signal. Since equation (31) holds, it was revealed that the phase angle does apply for a cosine wave instead of a sine wave. This is shown in Figure 68.

$$\sin(x + 90) = \cos(x) \quad (31)$$

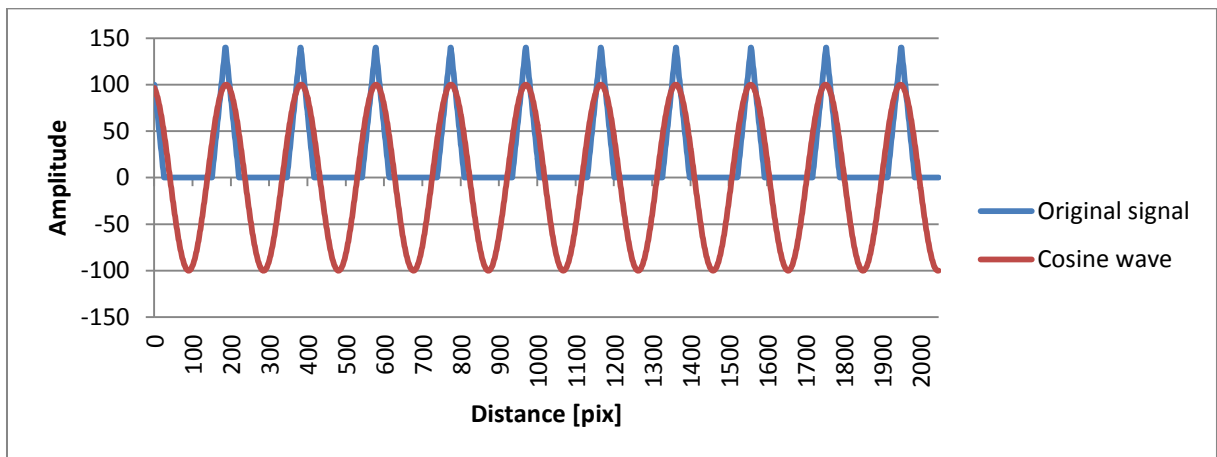


Figure 68: Signals from Figure 67, making use of a cosine wave instead of a sine wave (red line).

It can be seen from Figure 68 that f_e and φ_e were estimated correctly in order that the cosine wave does correspond to the original intensity graph. Since the original signal does not contain variation, only rounding errors caused that the peaks of the cosine wave should not correspond exactly to the peaks of the original intensity graph.

However, it was noticed that when $\varphi(n)$ was smaller than $\varphi(n + 1)$, the phase angle was not determined correctly anymore. When considering $F(u)$, this behaviour was also seen for $I(u)$. As an example the intensity graph of Figure 65 was used again, but with $hs = 60$ pix. This horizontal shift

ensures that the phase angle of the cosine wave changes. From the lower graph it is seen that $I(10)$ is smaller than $I(11)$.

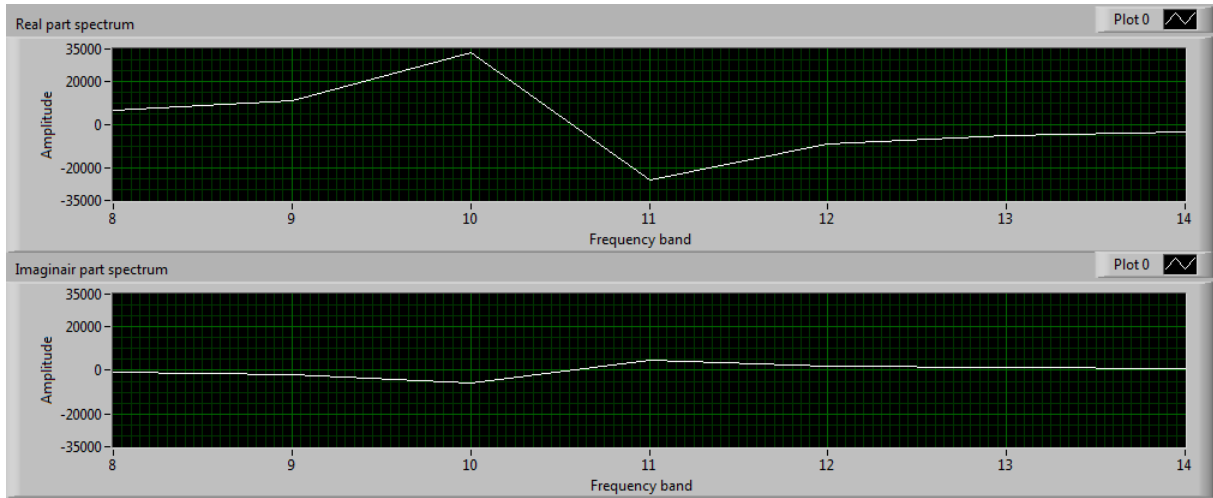


Figure 69: $R(u)$ (above graph) and $I(u)$ (below graph) of the intensity graph similar to Figure 65, but with a horizontal shift of the objects of 60 pixels to the right.

Calculating the resulted phase angle (φ_e) would have resulted in a non-corresponding cosine wave, which is demonstrated by the equations:

$$\varphi(10) = \arctan \left[\frac{-5671}{33289} \right] = -9.67^\circ$$

$$\varphi(11) = \arctan \left[\frac{4840}{-25776} \right] = 169.37^\circ$$

$$\varphi_e = 0.53 * -9.67 + 0.47 * 169.37 = 74.48^\circ$$

The resulting graph is shown in Figure 70. It is clear that in this graph the cosine wave and the original signal does not correspond.

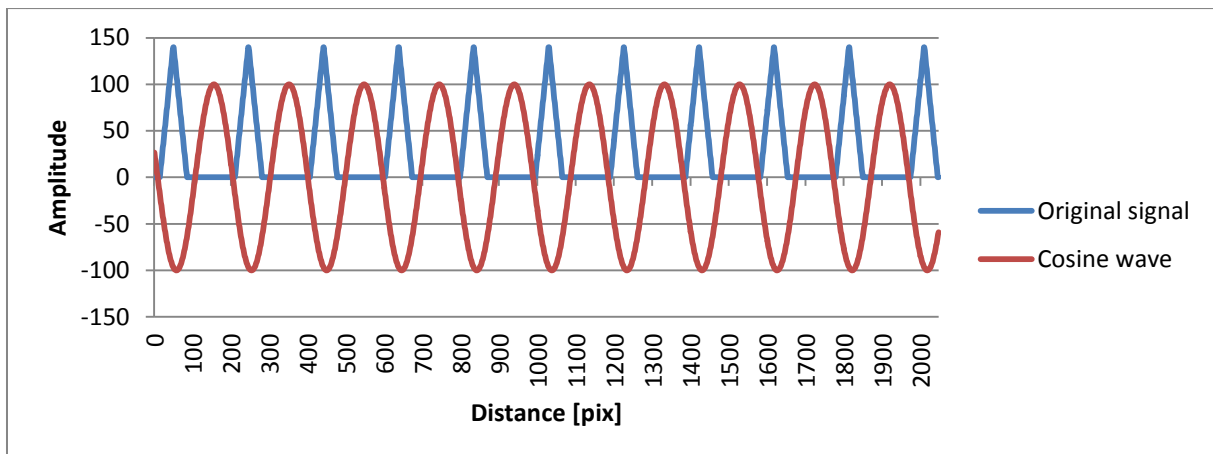


Figure 70: Original intensity graph from Figure 65 (blue line) overlaid with a cosine wave having frequency $f_e = 10.47$, phase angle $\varphi_e = 74.48^\circ$ and amplitude of 100 (red line).

Since the phase angle is a modulo value it is allowed to add up 360° to $\varphi(n)$ until $\varphi(n)$ is larger than $\varphi(n + 1)$. Figure 71 shows that $\varphi(10) + 360$ made that the cosine wave corresponds to the original signal.

$$\varphi_e = 0.53 * (-9.67 + 360) + 0.47 * 169.37 = 265.28^\circ$$

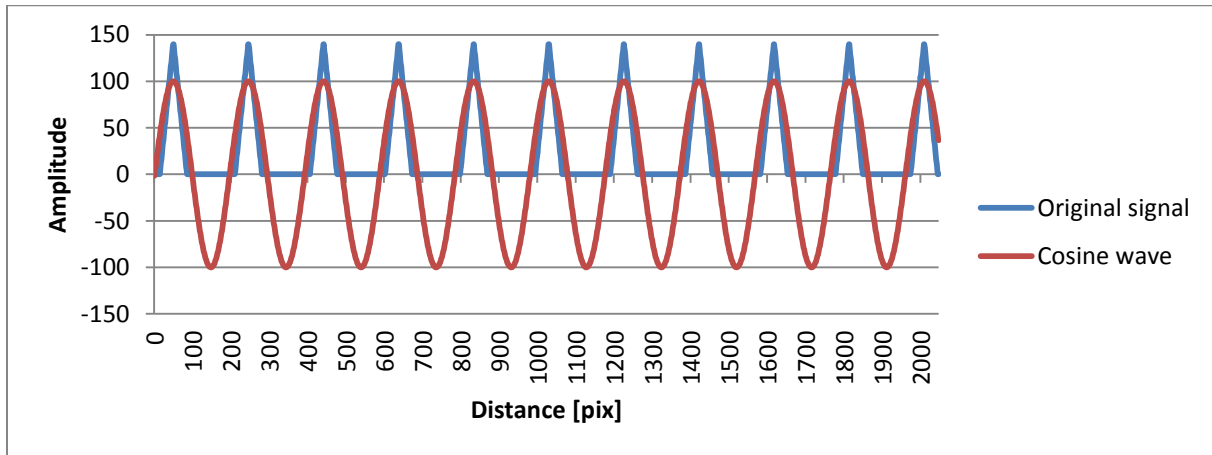


Figure 71: Original intensity graph from Figure 65 (blue line) overlaid with a cosine wave having frequency $f_e = 10.47$, phase angle $\varphi_e = 265.28^\circ$ and amplitude of 100 (red line).